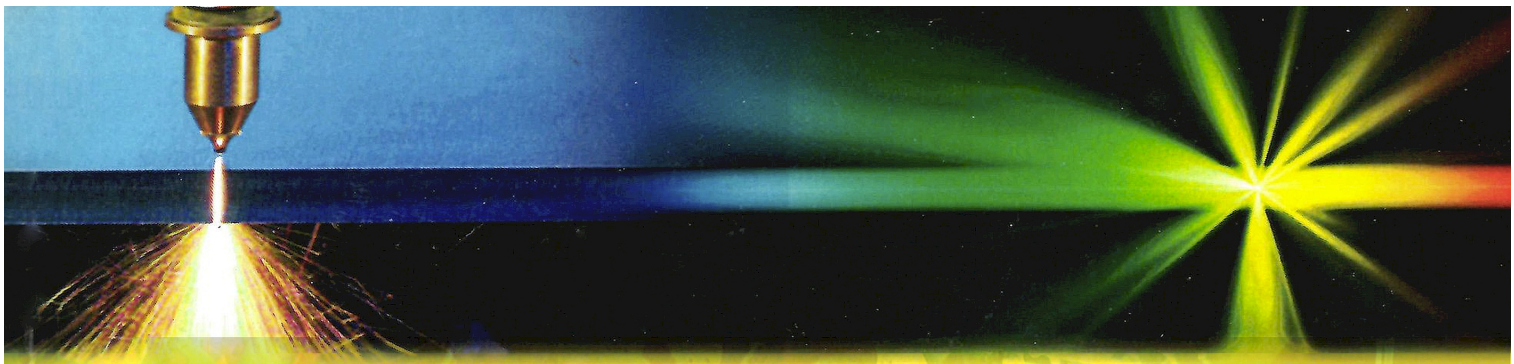


Ministry of Education and Science of Ukraine
Scientific Council on Laser Physics and Laser Technologies of NASU, Ukraine
Institute of Physics of NASU, Ukraine
V. Lashkarev Semiconductor Physics Institute of NASU, Ukraine
G. Karpenko Physical Mechanical Institute of NASU, Ukraine
Riga Technical University, Latvia
University of Rzeszow, Poland
I. Franko Drohobych State Pedagogical University, Ukraine

MATERIALS OF
SCIENTIFIC AND TECHNICAL CONFERENCE

LASER TECHNOLOGIES. LASERS AND THEIR APPLICATION

June 29 - June 30, 2023
Truskavets, Ukraine
https://ltla.pl
ONLINE

Ministry of Education and Science of Ukraine
Scientific Council on Laser Physics and Laser Technologies of NASU, Ukraine
Institute of Physics of NASU, Ukraine
V. E. Lashkarev Semiconductor Physics Institute of NASU, Ukraine
G. Karpenko Physical Mechanical Institute of NASU, Ukraine
Riga Technical University, Latvia
University of Rzeszów, Poland
Ivan Franko Drohobych State Pedagogical University, Ukraine

MATERIALS

OF INTERNATIONAL SCIENTIFIC

AND TECHNICAL CONFERENCE

LASER TECHNOLOGIES.
LASERS AND THEIR APPLICATION.

LTLA-2023

June 29 - June 30, 2023

Truskavets, Ukraine
Rzeszów, Poland

UDK 535.37(063)
ББК 22.3я43
M34

Materials are recommended for publication by the
by the Scientific Council of the
Institute of Physics National Academy of Sciences of Ukraine
(Protocol N5 on 25 Maj 2023)

Laser Technologies. Lasers and their Application (LTLA-2023):
Materials of International Scientific & Technical Conference.
- Drohobych. -
2023. - 48 p.

ISBN 978-966-384-345-2

The book contains the abstracts of International Scientific and Technical Conference «Laser technologies. Lasers and their application» for such scientific topics:

- Physical and mathematical fundamentals of laser systems.
- Development of lasers and laser systems.
- Laser processing of materials.
- Laser deposition.
- Laser technical and technology applications.
- Lasers in nanotechnologies.
- Biomedical laser applications.

The book will be useful for scientists and post-graduate students working in the field of physics and technology of lasers and laser technologies.

Address of conference: Ivan Franko Drohobych State Pedagogical University, Faculty of Physics, Mathematics, Economics and Innovation Technologies, 3 Stryjska Str., Drohobych, Lviv Region, 82100.
E-mail: laser-2023@ukr.net; isvirt@email.ua

Edited by
Dr. Sci., Prof. **V. Taranenko**,
Dr. Sci., Prof. **I. Stefaniuk**
Dr. Sci., Prof. **I. Virt**

The abstracts were printed as received, without any substantive corrections and at the responsibility of the authors.

SCIENTIFIC PROGRAM COMMITTEE

Chairmen prof. Taranenko V. Institute of Physics of the NASU, Ukraine
Chairmen prof. Stefaniuk I. University of Rzeszów, Poland
Chairmen prof. Virt I. Ivan Franko Drohobych State Pedagogical University, Ukraine
prof. Asmontas S. Semiconductor Physics Institute, Lithuania
prof. Bobitski Ya. Lviv Polytechnic National University, Ukraine
prof. Bilynskyi I. Ivan Franko Drohobych State Pedagogical University, Ukraine
prof. Cebulskii J. University of Rzeszów, Poland
prof. Druzhinin A. Lviv Polytechnic National University, Ukraine
prof. Duriagina Z. Lviv Polytechnic National University, Ukraine
prof. Fekeshgazi I. Uzhhorod National University, Ukraine
prof. Muravskyy L. Karpenko Physico-Mechanical Institute of the NASU, Ukraine
prof. Padlyak B. University of Zielona Góra, Poland
prof. Prokhorenko S. Lviv Polytechnic National University, Ukraine
prof. Stolyarchuk I. Ivan Franko Drohobych State Pedagogical University, Ukraine
prof. Tetyorkin V. V.E. Lashkaryov Institute of Semiconductor Physics of the NASU, Ukraine
prof. Vlokh R. Institute of Physical Optics of the NASU, Ukraine
prof. Voloshinovskii A. Ivan Franko National University of Lviv, Ukraine
prof. Wal A. University of Rzeszów, Poland
prof. Wnuk M. University of Rzeszów, Poland

ORGANIZING & LOCAL COMMITTEE

Prof. Virt I. – chairmen (UR);
Dr. Kuzyk O. – secretary (DSPU);
Dr. Potera P. – secretary (UR).

Members:
Dr. Adamiak S. (UR**), Cieniek B.** (UR), **Frolov S.** (IOP), **Dr. Lymarenko R.** (IOP), **Dr. Voitovych K. (**DSPU).

Contact address to:
prof. I. Virt, Faculty of Physics, Mathematics, Economics and Innovation Technologies, 3 Stryiska Str, Drohobych, 82100, Ukraine.
E-mail: *laser2023@ukr.net, isvirt@email.ua*
Website: https://ltla.pl

Topic I: Physical and mathematical fundamentals of laser systems:

- Mathematic modeling of radiant technologies;
- Interaction of highly concentrated energy currents with surface;
- Functional materials for laser equipment.

Laser elements based on dye-doped polyurethane matrices

A. Negriyko[1], V. Bezrodnyi[1], T. Bezrodna[1], L. Kosyanchuk[2], O. Antonenko[2]

[1] *Institute of Physics NAS of Ukraine, 46 Nauki av., 03028 Kyiv, Ukraine*
[2] *Institute of Macromolecular Chemistry NAS of Ukraine, 48 Kharkivske av., 02160 Kyiv, Ukraine*

Dye-doped polymers are prospective materials for optoelectronic devices, especially for a use in quantum electronics, electroluminescence, photovoltaic solar technology, information recording and storage. They enable transformation of the light radiation over a wide spectral range with higher efficiency, than polymers and dyes themselves. However, these advantages can be realized only in the case, when the polymer matrices do not essentially distort the spectral, luminescent and nonlinear optical properties of doping dyes.

As applied to quantum electronic devices based on organic dyes, solid-state matrices have operational advantages over liquid media. Among solid-state materials, polymers are most suitable due to their diversity, availability, low cost, structure homogeneity and possibility of easy introduction of dyes.

Complex investigations, carried out for many years at the Institute of Physics NAS of Ukraine have shown that polyurethane matrices, containing aliphatic and aromatic diisocyanates are promising for practical use as effective media in solid-state laser elements and laser devices based on organic dyes. Experiments with a use of dye-doped polyurethanes allowed developing and studying the following issues:

-passive Q-switching of solid-state lasers [1],

-passive mode-locking [2],

-generation of dye lasers [3],

-determination of dipole moments for the dyes in polymer matrices [4].

This work presents results on the developed synthesis method for the cross-linked optically transparent polyurethanes, based on hydroxyl-containing oligomers of different functionality and molecular weight and different type isocyanates, as well as on such polyurethane doping with the dyes of phenalenone, xanthene and pyrromethene classes. Effects of the polarity properties of polyurethane matrices on the spectral-luminescent and generation properties of laser active elements have been analyzed. The transition from aromatic to aliphatic polyurethane has caused the polarity increase, which contributes to the larger Stokes shift and lower luminescence quenching, as well as to the photostability improvement of the dye-doped active laser materials.

Carried out experimental research of laser elements based on colored polyurethane matrices makes it possible to develop efficient and stable solid-state devices for quantum electronics based on laser organic dyes.

[1] V.I. Bezrodnyi, A.A. Ishchenko, High-energy single pulse and multi-spike operation with a passive polymer Q-switch, *Opt. Laser Technol.*, 34 (2002) 7–13.

[2] T. Bezrodna, V. Bezrodnyi, A. Ishchenko, Yu. Slominskii, I. Sharanov, New polymethine dyes for liquid and polymer passive Q-switches of neodymium lasers, *Optik*, 267 (2022) 169725.

[3] T.V. Bezrodna, V.I. Bezrodnyi, A.M. Negriyko, L.F. Kosyanchuk, Spectral, photophysical and lasing properties of Rhodamine dyes in the polyurethane acrylate matrix, *Opt. Laser Technol.*, 138 (2021) 106868.

[4] T. Bezrodna, A. Negryiko, V. Bezrodnyi, L. Kosyanchuk, Dipole moments of phenalenone dyes determined in liquid and polymer polar media, *J. Mol. Liq.*, 267 (2018) 89–95.

Laser materials based on borate glasses, co-doped by Er and Ag

B.V. Padlyak[1,2], I.I. Kindrat[1], R. Lisiecki[3], V.T. Adamiv[2]

[1] *University of Zielona Góra, Institute of Physics, 4a Szafrana Str., Zielona Góra, 65-516, Poland*
[2] *Vlokh Institute of Physical Optics, 23 Dragomanov Str., Lviv, 79005, Ukraine*
[3] *Institute of Low Temperature and Structure Research of the Polish Academy of Sciences, Department of Spectroscopy of Laser Materials, 2 Okólna Str., 50-422 Wrocław, Poland*

The $Li_2B_4O_7$ glasses doped by Er and co-doped by Er and Ag were detailed studied by electron paramagnetic resonance (EPR), and optical spectroscopy [1,2]. The $Li_2B_4O_7$:Er and $Li_2B_4O_7$:Er,Ag glasses of high quality were obtained by conventional melting technology. The Er impurity was added to raw materials as Er_2O_3 of chemical purity (99.99 %) in amounts 0.5 and 1.0 mol.%. The Ag impurity was embedded to the glass composition as $AgNO_3$ and highly-dispersed metallic silver in amount 2.0 mol.%. The EPR and optical spectroscopy show that in the $Li_2B_4O_7$ glass network Er impurity is incorporated as Er^{3+} ($4f^{11}$, $^4I_{15/2}$) ions, exclusively, whereas the Ag impurity is incorporated as Ag^0 ($4d^{10}5s^1$, $^2S_{1/2}$), Ag^+ ($4d^{10}$, $^1S_0$), and Ag^{2+} ($4d^9$, $^2D_{5/2}$) ions and their aggregates (clusters). Optical absorption, photoluminescence (excitation and emission) spectra and decay kinetics of the Er^{3+} and Ag^+ single ions as well as Ag aggregates in the studied glasses were analysed [1,2].

Based on standard Judd–Ofelt theory the oscillator strengths (P_{cal}) and the experimental oscillator strengths (P_{exp}) of the observed absorption transitions as well as phenomenological intensity parameters (Ω_2, Ω_4, Ω_6) for Er^{3+} ions in the studied glasses were calculated. Spectroscopic parameters of relevance for laser applications, including emission probabilities of transitions (W_r), branching ratios (β), and radiative lifetime (τ_{rad}) were evalated for main observed emission transitions of the Er^{3+} ions in the $Li_2B_4O_7$:Er and $Li_2B_4O_7$:Er,Ag glasses. Experimental and calculated lifetime values for Er^{3+} ions in both studied glasses were compared and the quantum efficiency (η) for green ($^4S_{3/2} \rightarrow {}^4I_{15/2}$ transition, λ_{max} = 546 nm) and infrared (IR) ($^4I_{13/2} \rightarrow {}^4I_{15/2}$ transition, λ_{max} = 1530 nm) emission bands was calculated. Considerable increasing of quantum efficiency (~10 %) of the Er^{3+} green emission in the $Li_2B_4O_7$:Er,Ag glass [2] in comparison with $Li_2B_4O_7$:Er glass [1] was observed. The observed enhancement is attributed to excitation energy transfer from Ag^+ to Er^{3+} ions as well as local field effects induced by surface plasmon resonance of silver metallic nanoparticles. Potential applications of $Li_2B_4O_7$:Er and $Li_2B_4O_7$:Er,Ag glasses for visible and IR lasers are considered.

[1] B. V. Padlyak, R. Lisiecki, W. Ryba-Romanowski, *Opt. Mater.* 54 (2016) 126-133.

[2] I. I. Kindrat, B. V. Padlyak, R. Lisiecki, V. T. Adamiv, I. M. Teslyuk, *Opt. Mater*. 85 (2018) 238-245.

Enhancement of acousto-optic diffraction efficiency due to the ellipticity of optical eigenwaves caused by an external magnetic field and spontaneous electric polarization

O. Mys, D. Adamenko, I. Martynyuk-Lototska, and R. Vlokh

O.G. Vlokh Institute of Physical Optics, 23 Dragomanov Street, 79005 Lviv, Ukraine

The acousto-optic (AO) diffraction consists in interaction of light with a phase grating of refractive index created in a material medium due to elasto-optic (EO) effect. The efficiency of AO diffraction is characterized by a so-called AO figure of merit (AOFM) [1],

$$M_2 = \frac{n_i^3 n_d^3 p_{eff}^2}{\rho v^3},$$

which depends on the constitutive parameters of a AO material: the refractive indices of the incident (n_i) and diffracted (n_d) optical waves, the velocity v of acoustic wave (AW), the effective EO coefficient p_{eff}, and the density ρ.

When analyzing the influence of optical activity on the efficiency of AO diffraction in $Pb_5Ge_3O_{11}$ crystals, it is shown that its presence significantly increases the AOFM due to the nonzero ellipticity of the interacting optical eigenwaves induced by spontaneous electric polarization due to the effect of spontaneous electrogyration. At the same time, it was found that such an increase to one degree or another is characteristic of all types of AO diffraction and occurs due to the fact that the ellipticity of the optical eigenwaves approaches unity in the vicinity of the optical axis, and also because additional EO tensor components are included in the effective EO coefficient, taking into account the above-mentioned ellipticity [2].

Using the example of KDP crystals, which do not manifest the natural optical activity at the light propagation along the optic axis, for isotropic AO diffraction with a quasi-longitudinal (QL) AW, for the first time it was demonstrated that by induction of ellipticity of optical eigenwaves by an external magnetic field due to the Faraday effect the AOFM can be increased by approximately two times to a certain saturation value. Such an increase occurs when an external magnetic field is applied along the optical axis, subject to propagation of incident and diffracted optical waves in directions close to the optical axis with polarizations that coincide with those of magnetically induced polarizations of elliptical optical eigenwaves. These results show the fundamental possibility of controlling the efficiency of AO diffraction by means of an external magnetic field. Since the values of the external magnetic field strength required to achieve saturation of the AOFM depend on the corresponding Faraday-tensor components of the AO medium, the use of magnetically ordered materials for this purpose turns out to be particularly effective [3].

[1] L. Magdich and V. Molchanov, Acoustooptic devices and their applications, Philadelphia: Gordon and Breach Science Publisher, 1989.

[2] O. Mys, M. Kostyrko, D. Adamenko, I. Martynyuk-Lototska, I. Skab, and R. Vlokh, "Effect of ellipticity of optical eigenwaves on the enhancement of efficiency of acousto-optic Bragg diffraction. A case of optically active $Pb_5Ge_3O_{11}$ crystals," *AIP Adv.*, vol. 12, p. 055130, 2022.

[3] O. Mys, D. Adamenko, and R. Vlokh, "Influence of Faraday elliptical birefringence on the acousto-optic diffraction efficiency: a case of isotropic interaction with quasi-longitudinal acoustic waves in KH_2PO_4 crystals," *Ukr. J. Phys. Opt.*, vol. 24, p. 95–103, 2023.

Compact diode-pumped Nd:YAG laser.

I. Matsniev, V. Khodakovskyy, A. Negriyko

Institute of Physics NAS of Ukraine, 46 Nauky av., Kyiv 03028, Ukraine

We developed a laboratory sample of a pulsed solid-state laser with passive Q-switch modulation and pumping with semiconductor lasers with the aim of working out the domestic technology of creating individual elements of such a laser and the system as a whole. It was assumed to create samples of laser emitters with a set of qualities that satisfy needs beyond the capabilities of serial devices: autonomy, high energy and frequency of pulses, the ability to choose the mode of operation with high or low pulse energy, etc.

The active element of the laser (Nd:YAG) has the shape of a cylinder with 1.06 nm anti-reflection coated ends, the diameter of which is 6.3 mm and the length is 63 mm. Three laser diode bars from the company JENOPTIK Laser GmbH, Germany, model JOLD-300-QPNN-1L, are used in the transverse pump scheme, have an emission wavelength of 808 nm, a spectral width of the emission line of 3 nm, and an optical power of up to 300 W each. The laser bars are located with their emitting surfaces parallel to the side surface of the active element with a shift of 120 degrees in a circle. Also, they are shifted along the length of the active element. Q-factor of our laser was modulated by a passive laser shutter of a triplex design with AR-coated outer working surfaces. An active medium of our shutter is metal-organic complex of nickel dye dissolved in polyurethane composition matrix [1, 2].

The current driver provided the duration of the pumping pulses of 200..500 μs and the tracking frequency up to 100 Hz and up to 300 A peak amplitude. The temperature of each pump diode is stabilized separately with an accuracy of 0.1°C by a digital thermostat. The digital sensor provide the temperature data to the microcontroller, which, using the PID algorithm, calculates the duty cycle of the pulse width modulation of the current through the Peltier elements on which the laser diodes are mounted. The general power supply of the laser comes from a constant voltage in the range of 12..14 V, which makes it possible to power it from the on-board network of the car or a separate battery. The laser emitter and control equipment are combined into one block with dimensions of 200x300x170 mm.

For each individual shutter, when the pump current increases, a moment occurs when the radiation power accumulated in the active medium becomes sufficient to illuminate the shutter, and at the end of the pump pulse, one short optical pulse of high power appears at the output of the laser. The typical duration of such pulses (FWHM) is about 25 ns. As the pumping intensity increases, the number of such optical pulses increases, the laser generates a train of pulses. Studies conducted with various shutters and their combinations show that as the shutter's transmittance in the closed state decreases, the total energy of the laser pulse train also decreases, but the energy of each individual pulse increases. For example laser with 92% transmittance shutter provide 70 Q-switch pulses with 0,6 mJ of every pulse. Laser with 40% transmittance shutter provide 1 Q-switch pulse with 13,4 mJ energy. The peak power of this pulse slightly exceeds 500 kW.

[1] Безродный В. и др. “Новый наносекундный полимерный пассивный затвор для неодимовых лазеров” Квантовая электроника.-1995.- №3.- С. 245-248 .

[2] Безродный В. и др. “Исследование пассивной модуляции добротности Nd:YAG лазера с затворами на основе окрашенных полиуретановых матриц” Доповіді НАН України.- 2016.- №9.- С. 61-68.

M^2 measurement based on long range focusing of laser beam

A. Derzhypolskyi, L. Derzhypolska, A. Negriyko

Institute of Physics NAS of Ukraine, 46 Nauky av., 03028 Kyiv, Ukraine

M^2 known as laser beam quality factor or also a beam propagation ratio is a major parameter determining the behavior of commonly used lasers passing through optical systems and free space including focusing, collimation, divergence etc. The commonly established method of measurement of M^2 is regulated by ISO 11146 standard [1]. It relies on determination of laser beam diameter close to and around the beam waist with further non-linear fit of the measurement points to calculate M^2. There are also other methods used as more simple, like just measuring the beam waist and beam divergence, or more complicated involving beam profiling and wavefront analysis using Shack-Hartmann sensor. [2, 3]

In this work described is an alternative method of M^2 measurement based on long range laser beam focusing. The method relies on focusing the tested laser beam at different distances and measuring corresponding spot size. Further a linear fit is applied to measurement points to extract M^2 value. It is generally accepted that focusing of a laser beam is connected to formation of a beam waist, the narrowest part of a beam. However, as shown in the work in long range focusing there is a waist limit, i.e. the maximum distance at which the waist could be formed. Focusing at larger distances (getting the minimum possible spot size) is no longer related to beam waist. Furthermore, this is neither the case even at closer distances, where the beam waist yet could be formed [4]. Particularly, at waist limit the best focused beam spot is 2 times less than the waist size. Eventually, the best focused laser beam spot size is shown to be true linear with focusing distance, on the contrary to beam waist, and is always less than beam waist. This linear dependence leads to straightforward determination of M^2 with known wavelength and initial laser beam diameter. Theoretical considerations are given and experimental measurements of laser focusing at distances up to 1000m are presented. For laser spot diameter determination a D4σ method, also described in ISO 11146, is used and implemented in image processing code in MATLAB [...] environment. Another piece of MATLAB code is developed and applied for real time tracking of focused spot size at a given distance to catch a true minimum value.

[1] https://www.iso.org/standard/33625.html

[2] Bert John Neubert, Günter Huber, Wolf-Dieter Scharfe On the problem of M2 analysis using Shack-Hartmann measurements. Journal of Physics D: Applied Physics, Volume 34, Number 16, p.2414 (2001) DOI 10.1088/0022-3727/34/16/305

[3] A. E. Siegman, How to (Maybe) Measure Laser Beam Quality, in DPSS (Diode Pumped Solid State) Lasers: Applications and Issues, M. Dowley, ed., Vol. 17 of OSA Trends in Optics and Photonics, Optica Publishing Group, (1998), paper MQ1. https://web.archive.org/web/20110604095354/http://www.stanford.edu/~siegman/beams_and_resonators/beam_quality_tutorial_osa.pdf

[4] L. Derzhypolska, A. Derzhypolskyi and A. Negriiko, "Peculiarities of propagation and long distance focusing of expanded Gaussian laser beams," IEEE 8th International Conference on Advanced Optoelectronics and Lasers (CAOL), Bulgaria, pp. 1-4, (2019), doi:10.1109/CAOL46282.2019.9019577

Spectroscopy of the Tm-doped and Tm-Ag co-doped lithium tetraborate glasses

I.I. Kindrat[1], B.V. Padlyak[1,2], R. Lisiecki[3], A. Drzewiecki[1], I.M. Teslyuk[2], V.T. Adamiv[2]

[1] *University of Zielona Góra, Institute of Physics, Division of Spectroscopy of Functional Materials, 4a Szafrana Str., 65-516 Zielona Góra, Poland*

[2] *Vlokh Institute of Physical Optics, Department of Optical Materials, 23 Dragomanov Str., 79005 Lviv, Ukraine*

[3] *Institute of Low Temperature and Structure Research of the Polish Academy of Sciences, Division of Optical Spectroscopy, Laser Materials Spectroscopy Group, 2 Okólna Str., 50-422 Wrocław, Poland*

Spectroscopic properties of the Tm-doped and Tm-Ag co-doped borate glasses with $Li_2B_4O_7$ ($Li_2O–2B_2O_3$) basic composition have been investigated and analysed using optical absorption, electron paramagnetic resonance (EPR), and photoluminescence (emission, excitation, decay kinetics, quantum yield) techniques. The $Li_2B_4O_7$:Tm and $Li_2B_4O_7$:Tm,Ag glasses of high chemical purity and optical quality were obtained by standard glass melt-quenching technology [1].

Optical absorption spectra of the investigated glasses show several bands in the visible and infrared spectral ranges, which belong to the $4f – 4f$ transitions of Tm^{3+} ions from the $^3H_6$ ground state to the following excited states: $^3F_4$, $^3H_5$, $^3H_4$, $^3F_3$, $^3F_2$, and $^1G_4$. Optical absorption spectrum of the $Li_2B_4O_7$:Tm,Ag glass additionally shows a weak broad band attributed to the surface plasmon resonance (SPR) absorption of the silver nanoparticles. The EPR spectrum of the $Li_2B_4O_7$:Tm,Ag glass exhibits a broad unresolved signal with g_{eff} = 2.10 that belongs to the superposition of inhomogeneously broadened signals of the isolated Ag^0 and Ag^{2+} paramagnetic centres as well as their aggregates and nanoclusters.

The Tm^{3+} transitions were analysed in the framework of Judd–Ofelt theory. The oscillator strengths (f_{exp} and f_{cal}) and Judd–Ofelt intensity parameters (Ω_2, Ω_4, and Ω_6) were calculated. The radiative transition probabilities (A_{rad}), luminescence branching ratios (β), radiative lifetimes (τ_{rad}), and quantum efficiencies (η) of the Tm^{3+} emission transitions were estimated. Several Tm^{3+} transitions were identified as potential candidates for laser generation.

Luminescence spectra of the investigated glasses show intense blue ($^1D_2 \rightarrow {}^3F_4$ transition, λ_{max} = 452 nm), red ($^1G_4 \rightarrow {}^3F_4$ transition, λ_{max} = 650 nm), and infrared ($^3H_4 \rightarrow {}^3H_6$ transition, λ_{max} = 786 nm and $^3H_5 \rightarrow {}^3H_6$ transition, λ_{max} = 1.2 μm) emission bands. Luminescence excitation spectra show excitation bands related to transitions from the $^3H_6$ ground state to the $^1G_4$, $^1D_2$, $^1I_6$, $^3P_0$, $^3P_1$, and $^3P_2$ excited states of Tm^{3+} ions. The luminescence decay curves of the emission bands related to transitions from the $^1D_2$, $^1G_4$, and $^3H_4$ excited states of Tm^{3+} ions were detailed analysed and discussed. Besides this, luminescence spectra and decay curves of the Ag^+ ions and Ag aggregates in the $Li_2B_4O_7$:Tm,Ag glass were registered and discussed.

The enhancement of the Tm^{3+} luminescence in the $Li_2B_4O_7$:Tm,Ag glass was observed as a result of the energy transfer from Ag^+ isolated ions and Ag aggregates to the Tm^{3+} ions and local field effects induced by SPR of the silver nanoparticles. Based on the obtained results the possible applications of the investigated borate glasses are considered.

[1] I.I. Kindrat, B.V. Padlyak, R. Lisiecki, V.T. Adamiv, *J. Lumin.* 225 (2020) 117357.

Interlevel absorption of electromagnetic waves of the non-concentric spherical core-shell quantum dot

R.Ya. Leshko[1], I.V. Bilynskyi[1,2], O.V. Leshko[1]

[1] *Department of Physics and Information Systems, Drohobych Ivan Franko State Pedagogical University, St. Stryiska 3, Drohobych, 82100, Ukraine, e-mail: leshkoroman@gmail.com*
[2] *Physics Department, Kryvyi Rih State Pedagogical University,54 Gagarin Avenue, 50086, Kryvyi Rih, Ukraine*

New demands for the quality and performance of semiconductor structural elements used in electronics and optoelectronics are driven by the modern need for high-tech products. The creation of highly sensitive detectors capable of detecting various types of electromagnetic waves is relevant for both civil and military-industrial purposes. Quantum dots (QDs) have been used in the production of such detectors for some time now. Core-shell quantum dots are composite semiconductor nanoparticles consisting of a core material surrounded by a shell of a different material. Multilayer core-shell QDs offer significant potential and can be obtained through various methods, including colloidal solutions. However, technological processes and factors can result in non-concentric spherical QDs, where the core is displaced relative to the shell.

The unique electronic and optical properties of core-shell QDs are attributed to the confinement of charge carriers within the core, as well as the type and thickness of the shell material. While there is an established theory for concentric spherical multilayer QDs, the theory for non-concentric spherical core-shell QDs is underdeveloped. In this study, we developed a model of a non-concentric spherical core-shell QD using effective mass and the model of rectangular potential wells and barriers. We calculated one-electron energy spectra using numerical methods and established the dependence of electron energy on the size and degree of displacement of the nucleus from the center. Our theory shows that such a shift causes energy levels to split, leading to changes in the absorption of electromagnetic waves. According to the calculation, when the QD core is shifted from the common center, the energy levels split by $|m|$. This splitting is a result of lower symmetry caused by an increase in the displacement D. It has been demonstrated that the electron energy increases with the growth of displacements D.

The electron level dependence on core displacement D will influence the interlevel (intraband) coefficient of electromagnetic wave absorption, especially at the peak location. For example, linear polarization and circular polarization electromagnetic waves will be absorbed in different energies (when $D\neq0$) during 1s-1p interlevel transition, because the selection rule is $\Delta m=0$ (for linear polarization) and $\Delta m=1$ (for circular polarization). But 1p levels are split, therefore energy transitions will be different.

It has been showed that the core displacement D causes the changes of both electron and hole energy levels. That is why the effective band gap changes and it can bee seen on the interband absorption. We observed a shift of the main absorption band to the region of high energies when $D\neq0$.

The obtained features should be taken into account in the design of optical devices based on core-shell QDs. Also, the proposed theory can be extended to other multilayer QDs and QDs with impurities that may be developed in the future.

Stable color centers induced in $PbMoO_4$ crystals by gamma quanta irradiation

P. Potera[1], Ya. Zhydachevskii[2,3], D. Piwowarska[4], S.M. Kaczmarek[4]

[1] *Institute of Materials Engineering, College of Natural Science, University of Rzeszow University of Rzeszow, Rzeszow, Poland*
[2] *Lviv Polytechnic National University, Lviv, Ukraine*
[3] *Institute of Physics of the Polish Academy of Sciences, Warsaw, Poland*
[4] *Institute of Physics, West Pomeranian University of Technology, Al. Piastow 48, 70-310 Szczecin, Poland*

Lead molybdate crystal ($PbMoO_4$) is a well-known acoustooptical material with scheelite structure and have received recently much attention in the literature [1-4], due to for example the applications as Raman laser hosts. Such lasers can be space ships and be exposed to space radiation. For example the irradiation of oxide crystals by gamma quanta leads to the absorption changes in UV-Visible-near IR region [5]. In this way the study of radiation defects produced in gamma quanta in $PbMoO_4$ crystal is important.

The pure and Co doped $PbMoO_4$ crystals were grown by the Czochralski technique. The concentration of Co ions was 0,2 %. Samples for investigations were made in the form of plane-parallel polished plates of 0.9 mm thickness. The samples were irradiated with gamma quanta (1.25 MeV) from ^{60}Co with the absorbed dose of $3*10^4$ Gy. Optical absorption spectra were recorded with a Cary 5000 spectrophotometer. After measuring the additional absorption, the heating in air (by time 30 min in 423K and 723K) was performed by using a LHT 04/16 NABERTHERM furnace with C42 controller.

After irradiation pure $PbMoO_4$ crystal with gamma-quanta with dose of $3*10^4$ Gy, a broad additional absorption (AA) bands in the range of 27000 - 9000 cm^{-1} arise. The AA spectrum consists of three bands with maxima near 13200 cm^{-1}, 21100 cm^{-1} and 25000 cm^{-1}.

For the Co doped $PbMoO_4$ crystal a broad AA in the same region than for pure crystal with clear maximum near 23500 cm^{-1} and very slight maximum near 13000 cm^{-1} and 17600 cm^{-1} are observed, but intensity of AA is smaller than for pure crystal.

The centres responsible for AA absorption in pure and Co-doped crystals have limited thermal stability - annealing in air at 423 K for 30 minutes not change of absorption spectrum, but annealing at 723 K indeed restores the crystals to their original state.

According [2-4,6] the absorption changes in pure and Co doped $PbMnO_4$ crystals after gamma irradiation can be due to charge change of Mn, Fe and Pb ions and with appearance of F-type centers.

[1] H.C. Zeng, J. Cryst. Growth 171 (1997) 136-145.
[2] T.M. Bochkova, M.D. Volnyanskii, D.M. Volnyanskii, V.S. Shchetinkin, Phys. Solid State 45 (2003) 244.
[3] W. Bollmann, Kristall und Technik 15 (1980) 367-375.
[4] D. Piwowarska, S.M. Kaczmarek, P. Potera, P. Sagan, M. Berkowski, Optical Materials 31(12), (2009) 1798-1801
[5] A.Matkovskii, D.Sugak, S.Ubizskii, O.Shpotiuk, E.Chernyi, N.Vakiv, V.Mokritskii, Influence of ionizing radiation on electronic technique materials, Svit, Lvov, 1994 (in Russian)
[6] J.Y.Chen, Q.R.Zhang, T.Yu Liu, Z.X Schao, CH.Y. Pu, Chin. Phys. Lett, 24(6), (2007) 1660-1663

Topic II: Development of lasers and laser systems:

- Energy transfer dynamics in lasers
- Heat processes in lasers;
- Laser media development;
- Laser system modelling and optimization.

Stimulated UV Emission of ZnO Powder with Coherent and Incoherent Feedback

L. Fedorenko[1], D. Korbutyak[1], A. Evtukh[1], V. Naumov[1],
V. Yukhymchuk[1], P. Onufrijevs[2], A. Medvids[2], H. Mimura[3]

[1] *Lashkaryov Institute of Semiconductor Physics, National Academy of Sciences of Ukraine, Prospect Nauki 41, Kyiv 03028, Ukraine; e-mail: leonfdrn@gmail.com*
[2] *Institute of Technical Physics, Riga Technical University, Paula Valdena Str. 3/7, Riga LV-1048, Latvia; e-mail: medvids@latnet.lv*
[3] *Research Institute of Electronics, Shizuoka University, 3-5-1 Johoku, Naka-ku, Hamamatsu 432-8011, Japan; e-mail: mimura.hidenori@shizuoka.ac.jp*

The requirements of modern laser optoelectronics stimulates the search for new physical principles and approaches to increase the homogeneity of the laser field due to reducing the negative effect of speckles. In this regard, studies of disordered photonic media (DPM) with strong light scattering and high luminescence efficiency are very promising. One of the suitable DPM is based on ZnO crystallites [1]. In this work, we report on a comparative analysis of stimulated emission (SE) spectra of powdered ZnO DPM depending on the structure, size of crystallites and their distribution in ZnO powders. Based on studies of photoluminescence (PL) spectra, Raman shift, X-ray diffractograms and SEM images of different samples, the types of crystalline phases, the sizes of the smallest nanoparticles and their spatial distribution were determined. It was found that a polydisperse nano-micro-crystalline (PNMC) ZnO powder has particle sizes from 50 nm to 2 μm, which, in turn, consist of nanograins with a size of 25 nm. In the PL spectrum, this causes the maximum of the UV band at 387 nm to be fixed, and this explains the excitonic mechanism of SE in the entire excitation range. The superlinear growth of this excitonic band with the simultaneous narrowing of its half-width from 19 to 14 nm in PNMC ZnO powder indicates the SE with an incoherent feedback (FB). A fundamentally different evolution of the UV PL spectrum was observed in a monodisperse ZnO powder with an average nanoparticle (NP) size of 100 nm. In PL spectra, ultra-narrow peaks with a half-width of 0.2 nm were formed with a random spectral position and an irregular interval, which corresponds to the stochastic nature of the formation of microresonances in this DPM. It turned out that the superlinear growth of the UV PL occurs only for the integral intensity, which indicates the SE with a coherent FB. In the case of a thin-film ZnO DPM consisting of hexagonal microdisks, ultra-narrow peaks of the UV PL also appear, but with a regular spectral arrangement, which is due to SE with coherent FB in the gallery of whispering modes on the microdisk faces. An incoherent SE was established over the entire range of excitation intensities in the case of PNMC ZnO powder due to non-resonant lasing nature. The calculated amplification factor was about 150 cm^{-1}. The further development of research of incoherent SE sources based on ZnO powder in the direction of transition to 2D or 2D-like systems is justified [2].

[1] Cao, H.; Chriki, R.; Bittner, S.; Friesem, A.A.; Davidson, N. (2019) Complex lasers with controllable coherence. *Nat. Rev. Phys.* **1**, 156-168. https://doi.org/10.1038/s42254-018-0010-6.
[2] Lytovchenko, V.G.; Fedorenko, L.L.; Korbutyak, D.V.; Strikha, M.V. (2021) Ordered electron-hole condensate as a perspective 2D laser environment at room temperatures. *Ukr. J. Phys.* **66**, 612-617. https:/doi.org/10.15407/ujpe66.7.612.

Topic III: Laser processing of materials:

- Technological lasers;
- Laser technological system;
- Equipment for lasers and mixed technologies;
- Ablation, modification, annealing, precipitation, treatment and marking by laser bundle.

Anatase or Rutile TiO_2 Formation on Ti by Laser Radiation: Mechanical, Photocatalytic and Antibacterial Properties

A. Medvids[1], P. Onufrijevs[1], J. Kaupužs[1], J. Padgurskas[2], A. Zunda[2].

[1] *Institute of Technical Physics, Faculty of Materials Science and Applied Chemistry, Riga Technical University, P. Valdena 3/7, Riga, LV-1048, Latvia*
[2] *Institute of Power and Transport Machinery Engineering, Vytautas Magnus University, 11 Studentų Str., Kaunas LT-53362, Lithuania*

A laser-induced oxidation method for the formation of a TiO_2 layer on a Ti substrate was used. The TiO_2 phase can be controlled by an Nd:YAG laser with basic frequency at an intensity I=52.8 MW/cm^2 and three different doses: D1=3.1x10^{20} phot/cm^2, D2=3.9x10^{20} phot/cm^2, and D3=5.4x10^{20} phot/cm^2. Optical microscope image is in figure. Dose D1=3.1x10^{20} phot/cm^2 forms a TiO_2 layer in the anatase phase, which possesses the highest photocatalytic, antibacterial and adhesion properties. As the laser dose increases, the TiO_2 layer thickness increases from 40 nm to 100 nm, but the photocatalytic decomposition reaction constant decreases. The observed super-linear increase of the TiO_2 layer thickness with the laser dose is explained by the presence of positive feedback during the irradiation process. The temperature rises with increasing of the thickness due to the interference-caused decrease of the reflection coefficient.

As the thickness increases, TiO_2 on Ti structure adhesion decreases from 800 mN to 400 mN due to the formation of a layer with a mixture of phases. The colonization intensities of P. Aeruginosa and S. Epidermidis bacteria decrease more than tenfold after TiO_2 formation. These results are explained by the partial transformation of the TiO_2 layer, formed in the anatase phase at dose D1, into the rutile one at doses D2 and D3 due to a deficit of O atoms caused by the low diffusion of O atoms in Ti. According to our experiments and calculations, using the Wagner oxide model, the laser technology can be used to form crystalline structures with a monolayer precision.



Figure 1. Optical microscope image of TiO_2/Ti structure after irradiation by the laser doses D1, D2, and D3 at laser intensity 52.8 MW/cm^2.

EMR study of the $Fe_{73.5}Si_{15.5}B_7Nb_3Cu_1$ amorphous ribbon modified by laser

Yu. Nykyruy[1], B. Cieniek[2], I. Stefaniuk[2], S. Mudry[1]

[1] *Ivan Franko National University of Lviv, Metal Physics Department, Kyrylo and Mephodiy 8, Lviv, Ukraine*

[2] *Institute of Materials Engineering, College of Natural Science, University of Rzeszow, Pigonia 1, Rzeszow, Poland*

Amorphous $Fe_{73.5}Si_{15.5}B_7Nb_3Cu_1$ alloy was produced by the melt-quenching method in the form of a ribbon 25 mm wide and ~30 μm thick. A fiber laser (YAG:Nd, wavelength – 1060 nm) was used to modify the ribbon surface. Laser irradiation was performed in a continuous mode.

Electron magnetic resonance (EMR) method was used to study the amorphous $Fe_{73.5}Si_{15.5}B_7Nb_3Cu_1$ ribbon, as-cast and after laser irradiation. The EMR measurements were performed by Bruker multifrequency and multiresonance FT-EPR ELEXSYS E580 spectrometer. The angular dependence of EMR spectra was observed (Figure 1).

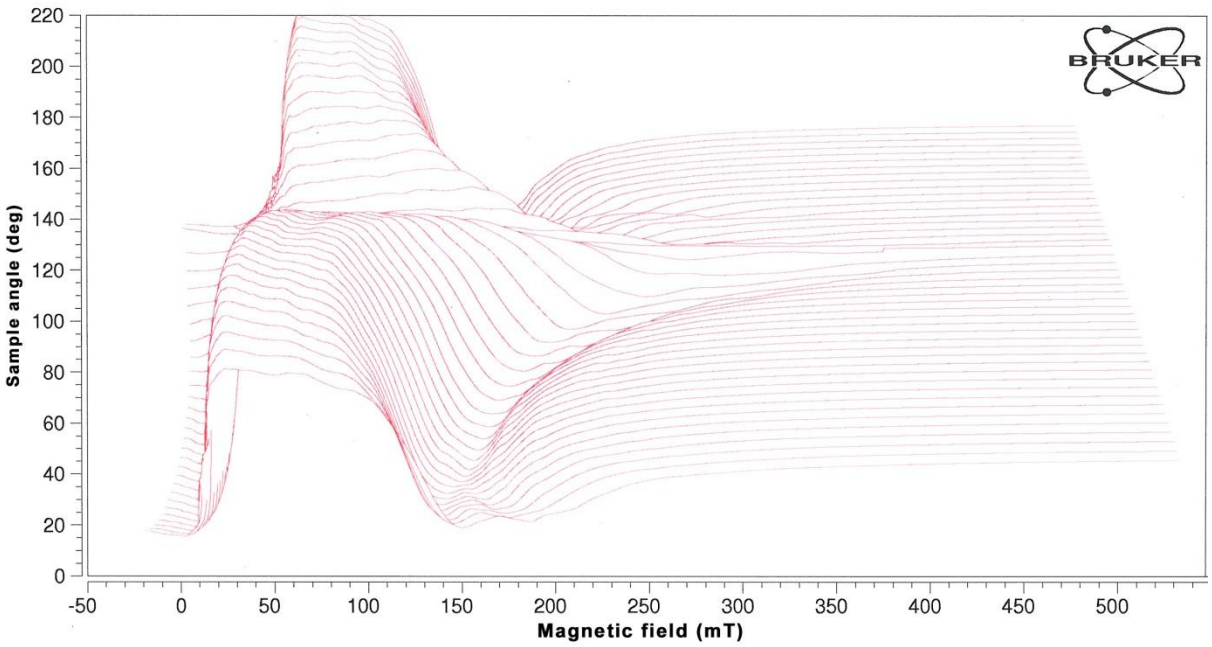


Fig. 1. Angular dependence of EMR spectra of $Fe_{73.5}Si_{15.5}B_7Nb_3Cu_1$ amorphous ribbon irradiated by laser.

The effect of laser radiation on the properties of paint components, studied using the EMR method.

W. Żyłka, B. Cieniek, I. Stefaniuk

Institute of Materials Engineering, College of Natural Sciences, University of Rzeszow, Pigonia 1, 35-310 Rzeszow, Poland

Electron magnetic resonance (EMR) spectroscopy is the best nondestructive method for testing paint components. EMR can detect any species with paramagnetic electrons, including organic and inorganic radicals, transition metal complexes [1], metalloproteins, and biradicals. EMR spectroscopy has been used to study rock paintings [2], wall paintings [3], and individual pigments [4,5]. This article presents an EMR study of the degradation of paint components under laser radiation. Measurements were carried out to evaluate the durability of pigments exposed to laser light. The parameters of the EMR line and the g-factor were determined. Electron magnetic resonance is the best method for evaluating paint components during laser light irradiation.

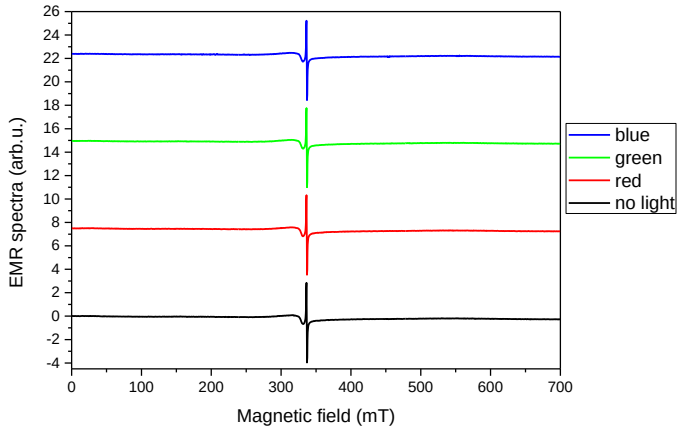


Figure 1. EPR spectra of 2K acrylic paint, purple pigment paste, effects of laser radiation at different wavelengths

References

[1] Stefaniuk, I.; Cieniek, B.; Virt, I. Magnetic Properties of Zinc-Oxide Composite Doped with Transition Metal Ions (Mn, Co, Cr). *Curr. Top. Biophys.* **2010**, *33*, 221–226.

[2] Rowe, M.W. Dating of rock paintings in the Americas: A word of caution. *CLOTTES J. (dir.), L'art pléistocène dans le monde / Pleistocene art world / Arte pleistoceno en el mundo, Actes du Congrès IFRAO, Tarascon-sur- Ariège, Sept. 2010, Symp. « Art pléistocène dans les Amériques ». N° spécial Préhistoire, Ar* **2012**, *LXV–LXVI*, CD573–CD584.

[3] Moretto, L.M.; Orsega, E.F.; Mazzocchin, G.A. Spectroscopic methods for the analysis of celadonite and glauconite in Roman green wall paintings. *J. Cult. Herit.* **2011**, *12*, 384–391, doi:10.1016/j.culher.2011.04.003.

[4] Christiansen, M.B.; Sørensen, M.A.; Sanyova, J.; Bendix, J.; Simonsen, K.P. Characterisation of the rare cadmium chromate pigment in a 19th century tube colour by Raman, FTIR, X-ray and EPR. *Spectrochim. Acta - Part A Mol. Biomol. Spectrosc.* **2017**, *175*, 208–214, doi:10.1016/j.saa.2016.12.028.

[5] Żyłka, W.M.; Cieniek, B.; Skała, P. Electron magnetic resonance study of the most sensitive metal paint components for degradation. *Adv. Sci. Technol. Res. J. 17*, 101–109.

Topic IV: Laser deposition:

- Modeling of laser deposition processes;
- Pulsed laser deposition;
- Equipment for plume laser deposition;
- Deposition of thin films and film structures.

Spectroscopic properties of nickel ions in $Zn_{0.99}Ni_{0.01}O$ thin film grown using PLD method

B. Cieniek[1], I. Virt[2,3], I. Stefaniuk[1]

[1] *Institute of Materials Engineering, College of Natural Sciences, University of Rzeszow, Pigonia 1, 35-310 Rzeszow, Poland*
[2] *Institute of Materials Engineering, College of Natural Science*
[3] *Department of Physics and Information Systems, Drohobych Ivan Franko State Pedagogical University, Stryiska 3, 82100 Drohobych, Ukraine*

Thin films of zinc oxide (ZnO) doped with nickel (Ni) exhibit interesting spectroscopic properties that can find applications in various fields. In optoelectronics Ni-doped alters the bandgap of ZnO, allowing for the absorption and emission of light in a wider range of wavelengths. This property makes it suitable for applications such as light-emitting diodes (LEDs) and displays [1]. Also, Ni-doped ZnO thin films can be utilized in gas sensors [2]. The spectroscopic properties of the material enable the detection and measurement of specific gases. By monitoring the changes in the optical or electrical properties of the material upon exposure to target gases, it is possible to create sensitive and selective gas sensing devices. Furthermore, the introduction of nickel ions into ZnO can lead to the development of magnetic properties in the material. This opens up opportunities for applications in spintronics, magnetic storage devices, and magnetic sensors. Electron paramagnetic resonance (EPR) has been used to study and characterize the magnetic, structural and spin properties of materials [3].

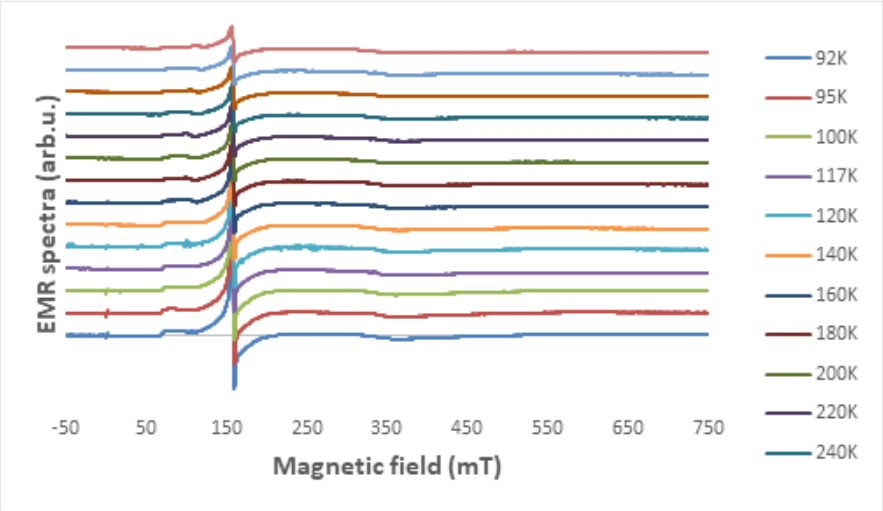


Figure 1. Temperature dependence of EMR spectra of $Zn_{0.99}Ni_{0.01}O$ thin layer

References

[1] Pearton, S.J.; Ren, F. Advances in ZnO-based materials for light emitting diodes. *Curr. Opin. Chem. Eng*. 2014, *3*, 51–55.
[2] Aleksanyan, M.; Sayunts, A.; Aroutiounian, V.; Shahkhatuni, G.; Simonyan, Z.; Shahnazaryan, G. Gas Sensor Based on ZnO Nanostructured Film for the Detection of Ethanol Vapor. *Chemosensors* **2022**, *10*, 245, doi:10.3390/chemosensors10070245.
[3] Borysiewicz, M.A. ZnO as a functional material, a review. *Crystals* **2019**, *9*, 505, doi:10.3390/cryst9100505.

Self- aggregated nanoparticles of ZnCrTe formed by laser ablation

A. Barlowski[1], P. Ciupak[1], K. Zembrowska[2], P. Sagan[3], T. Jasinski[1], M. Kuzma[2]

[1] Department of Physics and Medical Engineering, The Faculty of Mathematics and Applied Physics, Rzeszow University of Technology, al. Powstańców Warszawy 6, 35-959 Rzeszów, Poland;
[2] Technical College, East European State University in Przemyśl, Książąt Lubomirskich 6, 37-700 Przemyśl, Poland;
[3] The Faculty of Mathematics, Physics, and Computer Science, Maria Curie-Skłodowska University Lublin, plac Marii Curie-Skłodowskiej 5, 20-400 Lublin, Poland;

The ZnCrTe is a very promising new magnetic semiconductor while its Curie temperature exceeds the room temperature [1].

Nanoparticles of ZnCrTe were obtained by laser ablation. The laser YAG;Nd^{3+} with the energy of 0.8 J in a pulse was used. The pulse duration was 40 ns. The ablation was performed with second harmonic i.e. λ =532 nm in vacuum of 10^{-6} mmHg. The target was prepared from powders of the Cr_2Te_3 (Alfa Aesar) mesh 100 and of the Zn (Alfa Aesar) mesh 50, pressed into pallets with diameter of 5 mm. The weight of the constituent powders were matched to ensure the composition x = 0.75and x = 0.16 of the pellets of $Zn_{1-x}Cr_xTe$. Two kinds of substrates were selected; mirror polished single crystal Si and cleaved single crystal NaCl.

Usually, pulsed laser deposition results in polycrystal thin layers, single crystal thin layers or in three-dimensional species (e.g. pyramids) uniformly deposited on the surface. In our experiment we have obtained an aggregates of species in the form of uniform balls. The shape of aggregates is such as random fractals of the DLA type (Diffusion Limited Aggregation) [2]. In Fig. 1 we present typical SEM images of the aggregates.

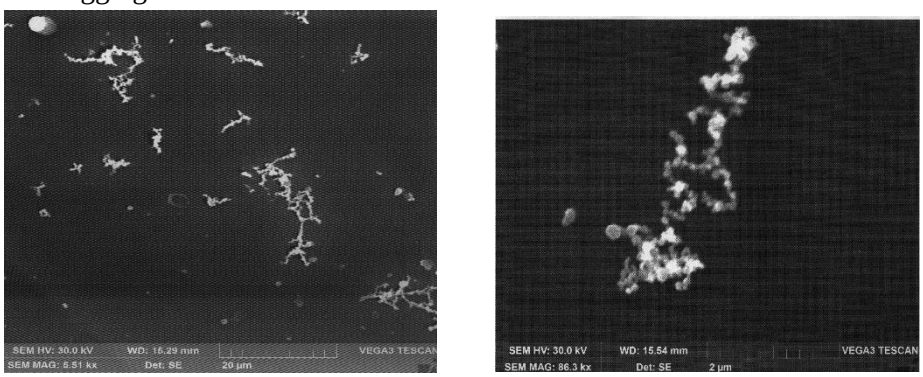


Fig. 1. SEM images of ZnCrTe aggregates on Si surface obtained by PLD.

The particles' size distribution was found to be relatively narrow. The mean diameter of these particles is d=100 nm.

The chemical composition was determined by EDS measurements.

References

[1] V. Tiwari, M. Arino, S. Gupta, M. Morita, T. Inoue, D. Caliste, P. Pochet, H. Boukari, S. Kuroda, and L. Besombes, Hole-Cr+ nanomagnet in a semiconductor quantum dot, Phys. Rev. B 104**,** L041301 **(**2021**).**

[2] H.O. Peitgen, H. Jurgens, D. Saupe, Introduction to Fractals and Chaos, Springer 2003.

Pulsed laser deposition of carbon nanotube films

I. Virt[1,2], P. Potera[3], B. Cieniek[3]

[1] *Department of Physics and Information Systems, Drohobych State Pedagogical University I.Franko, Drohobych, Ukraine;*
[2] *Institute of Physics, College of Natural Sciences, University of Rzeszow, Rzeszow, Poland;*
[3] *Institute of Materials Engineering, College of Natural Science, University of Rzeszow, Rzeszow, Poland*

Today, PLD technology is of great interest in industries such as microelectronics, micro- and nanophotonics, as obtaining high-quality film structures is a priority in these areas. Neodymium YAG: Nd laser was used in our experiment. The films SWCNTs (single-walled carbon nanotubes) were obtained in two ways. The first method is to spray the film in a vacuum. To do this, place the substrate (glass, silicon, quartz) on a platform in a vacuum chamber on which the films will be sprayed. The crystal structure of all MWNT layers before and after heat treatment (annealing at 400 °C for 10 min) was determined by X-ray phase analysis, mainly on silicon substrates. Microstructure studies by X-ray diffraction and SEM showed that the synthesized nanotubes were quite uniform in diameter and formed bundles of 5-20 nm in size. Clear peaks are observed, in particular, at angles 27°, 42° and 92° 2θ. Scanning electron microscope images were obtained for annealed and unheated samples. The nanographite domains are clearly visible in the SEM images, while the distance between nanotube layers can be estimated to be about 0.5 nm. The lateral size of the ordered regions is 10 nm. There is also a cluster of carbon nanospheres (NSCs), the size of which varies with changes in substrate temperature. Agglomerates with an average size of ~40 nm were observed.

For the analysis of films, their absorbency was measured in the wavelength range of 200-3000 nanometers on a spectrometer. The absorption capacity of light is characterized by a coefficient called absorption A (this is the product of the absorption coefficient by the film thickness). Absorption is determined by the ratio of light intensity (in particular, input I0 and output I). That is, $\ln (I/I_0) = A$, the parameter depends on the wavelength of light. If the absorption is represented not by the wavelength but by the energy of the photons of light, we can estimate the energy of the photons of light at which there is a sharp diffusion of light. absorbing layer. This physical effect is one of the methods of identifying both the material and its structure. Comparing with the literature [1,2], we can say that the resulting thin carbon film has one of the structural modifications of the graphene-like structure. The carbon nanoparticle powder was poured on a substrate (glass plate). However, it is known that the presence of a surface film of graphene leads to an increase in the microhardness of the material. Therefore, we measured the microhardness on a clean glass surface and on a film surface. Therefore, it can be assumed that the film obtained on the glass surface may have a graphene-like structure.

Therefore, it can be assumed that the film obtained on the glass surface may have a graphene-like structure. This physical effect is one of the methods to identify both the material and its structure.

[1] A.S.Saleemi, M.Hafeez, M.Saeed, A.Abdullah, M.Anis-ur-Rehman, and S.-L.Lee1 “Substrate Impact on MR Characteristics of Carbon Nano Films Explored via AFM and Raman” Analysis Materials (Basel), 14(13): 3649 (2021).

[2] K.B.Masood, P.Kumar, M. A.Malik, J.Singh “A comprehensive tutorial on the pulsed laser deposition technique and developments in the fabrication of low dimensional systems and nanostructures” Emergent Materials, V. 4, P. 737–754 (2021).).

Spectroscopic properties of nickel ions in $Zn_{0.9}Cu_{0.1}O$ thin film grown using PLD method

B. Cieniek[1], I. Virt[2,3], I. Rogalska[1,4], I. Stefaniuk[1]

[1] *Institute of Materials Engineering, College of Natural Sciences, University of Rzeszow, Pigonia 1, 35-310 Rzeszow, Poland*

[2] *Institute of Physics, College of Natural Sciences, University of Rzeszow, Rzeszow, Poland*

[3] *Department of Physics and Information Systems, Drohobych Ivan Franko State Pedagogical University, Stryiska 3, 82100 Drohobych, Ukraine*

[4] *International Centre For Interfacing Magnetism And Superconductivity With Topological Matter, Institute of Physics Polish Academy of Sciences, Lotników 32/46, 02-668 Warsaw, Poland*

Thin films of zinc oxide (ZnO) doped with copper (Cu) exhibit interesting spectroscopic properties that can find applications in various fields. In photocatalysis, the addition of copper modifies the energy band structure, enhancing the efficiency of photocatalytic processes. This can be beneficial for the removal of organic pollutants or the degradation of toxic substances in water or air. Also, Cu-doped ZnO thin films can be utilized in solar energy, and as gas detectors. Furthermore, Copper doping can influence the magnetic properties of ZnO, opening up possibilities for its utilization in spintronics. Spintronics utilizes electron spins for the transfer, storage, and manipulation of information. ZnO:Cu materials can be employed in the production of spin transistors, tunnel diodes, and other spin-based electronic devices. Electron paramagnetic resonance (EPR) has been used to study and characterize the magnetic, structural and spin properties of materials.

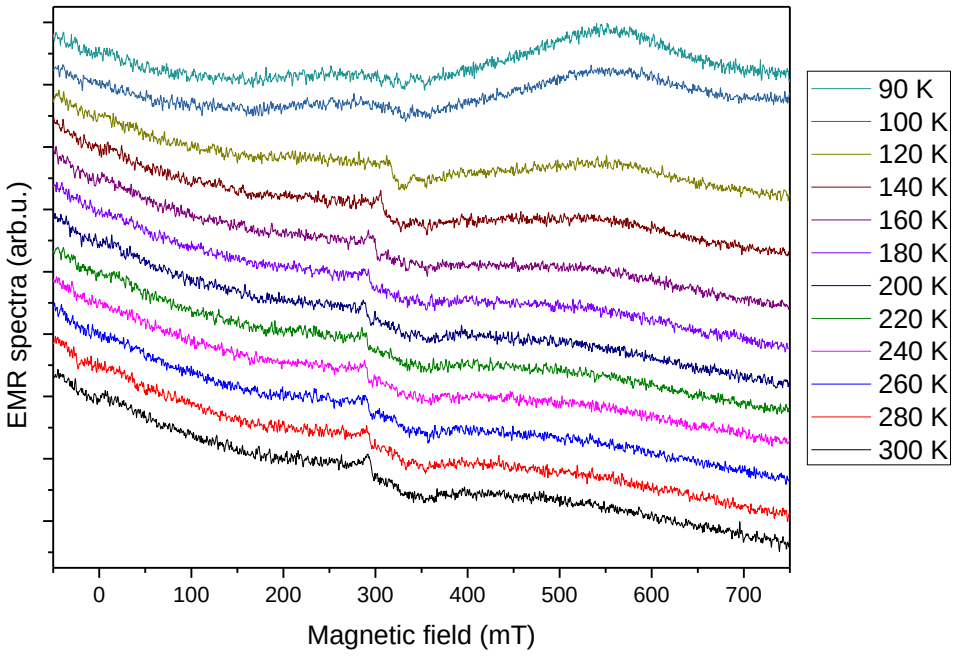


Figure 1. Temperature dependence of EMR spectra of $Zn_{0.9}Cu_{0.1}O$ thin film

Topic V: Laser technical and technology applications:

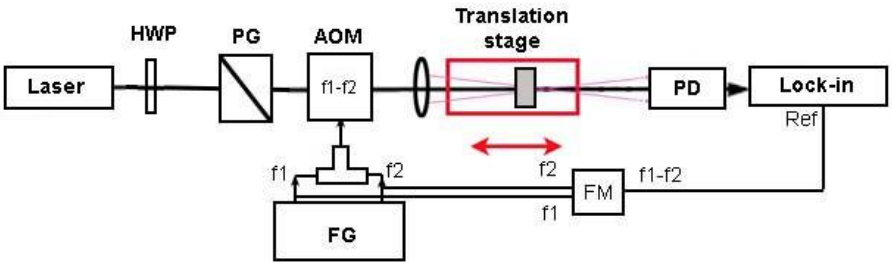
- Diagnostics on the basic of laser transmitters;
- Laser gauges;
- Laser lithography;
- Optoelectronic laser systems.

Sensitive measurements of two-photon absorption in semiconductors by combining Z-scan and loss modulation

V. Kadan[1,2], I. Pavlov[1,2], I. Blonskyi[1], T. Pavlova[2], Yu. Seriozhkin[3], A. Dmytruk[1]

[1] *Institute of Physics of NAS of Ukraine, Kyiv 03028, Ukraine*
[2] *Department of Physics, Middle East Technical University, Ankara 06800, Turkey*
[3] *V. Lashkaryov Institute of Semiconductor Physics of NAS of Ukraine, 41 pr. Nauky, 03028, Kyiv, Ukraine*

One of the most important parameters, strongly influencing the processes of laser machining and modification of semiconductor-based optoelectronic devices, is coefficient β of two-photon absorption (2PA), because namely 2PA is the main mechanism allowing to deposit precise portion of laser energy to exact positions inside the semiconductor material. Loss modulation technique for the measurement of β, proposed for the first time in [1], offers much higher sensitivity ($\beta \sim 10^{-6}$ cm/GW) in comparison with the traditional Z-scan. The modulation loss manifests itself in the appearance of second harmonics (SH) in the frequency spectrum of the transmitted laser beam, which originally is modulated by a pure sinusoid. Sinusoidal modulation was obtained in [1] by combining two beams of different frequency from the same femtosecond laser, which are frequency-shifted with two acousto-optic modulators and carefully combined in space and time with a delay line. We have used only one AOM, driven at two frequencies of 49,7 MHz and 50 MHz that differ by 30 kHz. Thus, we not only simplified and reduced the cost of the circuit, but also simplified its adjustment. The 30 kHz frequency is used as a reference for the lock-in amplifier. To take into account the spurious signal at 2*f* frequency of 60 kHz, appearing in a single AOM due to third-order intermodulation products [2], we record the SH signal while simultaneously scanning the tested sample in Z-direction. Thus we can extract the useful signal even from the high spurious SH. The level of the spurious signal was also reduced to 0.15% (compare with 25% in [1]) by using maximum laser power (2 W) beam and minimum AOM diffraction efficiency (1%). Home-made femtosecond fiber laser (pulse energy 2 μJ, duration – 350 fs, wavelength – 1030 nm, pulse repetition rate – 1 MHz, average beam power up to 2 W) was used in the experiment.



Our test measurements of nonlinear absorption in crystal Si demonstrate, that only 1 mW of average power of AOM output beam is needed to obtain 2PA signal despite the presence of linear absorption at 1030 nm. Moreover, a signal of third harmonics at 90 kHz, characterizing three-photon absorption coefficient, was also recorded. The possibility of measuring three-photon absorption in the presence of strong two-photon absorption is a unique new feature of the proposed method. The work on calibration the setup is underway. The work is supported by the Scientific and Technological Research Council of Turkey (TUBITAK), BİDEB-2221.

[1] P. Tian, W.S. Warren, OPTICS LETTERS **27** (2002) 1634-1636
[2] D. Hecht, IEEE Trans. Sonics Ultrason. **SU-24**, 7 (1977)

Determining the size and depth of square planar subsurface defects in laminated composites by optoacoustic technique

L. Muravsky, Z. Nazarchuk, O. Kuts

Karpenko Physico-Mechanical Institute of the NAS of Ukraine, Lviv, Ukraine

A new method is proposed for determining the size and depth of square planar subsurface defects in composite panels using the spatial structure of optical responses obtained at the fundamental and multiple resonant frequencies of the ultrasonic (US) radiation that excites the panel. The method is based on a new approach to detecting subsurface defects by producing dynamic speckle images of an excited area of the composite surface using an optical system [1]. This area can be treated as a region of interest (ROI) located directly above the defect. Under the action of ultrasonic excitation of the composite, a region of interest (ROI) is formed directly above the square defect, the oscillations of which are synchronous with the oscillations of the US wave. The ROI can be considered as a thin square clamped membrane, the mode structure of which oscillations is known both for the fundamental and for multiple resonant frequencies and its oscillations are synchronous with the oscillations of the US wave.

Flexural US waves generated in the thin composite structures and acting on the material in the direction transverse to the direction of propagation lead to the ROI vibrations at its resonant frequencies. Generation of a spatial optical response from a subsurface defect occurs due to the inclination of the transverse nodes of the ROI, which stand out in the response in the form of bright spots [1]. By comparing the spatial structure of the response with the mode structure of a square membrane, one can determine whether the resonant frequency is fundamental or multiple. The dimensions of the obtained optical response correspond to the dimensions of the defect. Knowing the size of the response and the value of the fundamental resonant frequency of the ROI f_{11}, the depth of the defect is determined from the series of experimental graphical dependences of the fundamental resonant frequency on the size of planar square defects. To reduce the error in determining the subsurface defect depth, series of multiple resonance frequencies f_{12}, f_{13}, f_{14}, f_{21},… on the size of the defects are additionally built. Similar dependencies can be constructed for rectangular, round, elliptical and other flat defects. The experimental results indicate discrepancies with respect to the theoretical ones, especially at a low defect depth of less than 0.4 mm. The identified discrepancies can be explained, in particular, by inaccuracies in the planar defects fabrication, limited panel sizes, deviations in the direction of US wave generation, as well as existing shear deformations and circular inertia of rotation caused by US excitation.

Experiments with fiberglass composite panels containing square defects 5–60 mm size, located at depths from 0.4 to 3 mm, were performed using the hybrid optical-digital system (HODS) experimental breadboard resistant to external vibrations. This system is much simpler than similar electronic speckle pattern interferometry and shearography systems because it does not have a reference beam. In addition, decorrelation and blurring of speckle patterns are used to detect defects in HODS, while decorrelation in interferometric systems makes it impossible to detect defects already at surface displacements of several tens of microns. Therefore, the proposed approach can detect larger defects than is possible using approaches based on speckle interferometry and shearography [2]. The optoacoustic systems and devices built on basis of the HODS can be used both in laboratory and natural conditions.

[1] Nazarchuk ZT, Muravsky LI, Kuts OG (2022) Nondestructive testing of thin composite structures for subsurface defects detection using dynamic laser speckles. Res Nondest Eval 33(2):59–77.
[2] Fomitchov PA, Krishnaswamy S (1997) A compact dual-purpose camera for shearography and electronic speckle-pattern interferometry. Meas Sci Technol 8(5):581.

Laser induced photoresponse in perovskite solar cells

S. Ašmontas, A. Čerškus, J. Gradauskas, A. Grigucevičienė, R. Juškėnas, K. Leinartas, A. Lučun, O. Masalskyi, M. Mujahid, K. Petrauskas, A. Selskis, A. Sužiedėlis, E. Širmulis,

Center for Physical Sciences and Technology, Saulėtekio av. 3, LT-10223 Vilnius, Lithuania (edmundas.sirmulis@ftmc.lt)

Metal halide perovskites are widely used in optoeletronics devices such as photodetectors, LEDs and perovskite solar cells (PSCs). Rapid progress in the field of PSCs has made it posible to achieve approximately 25% energy conversion efficiency at present time [1]. However, the problems of stability and reproducibility of PSCs parameters have not been fully resolved until now and therefore research on perovskite structures remains relevant.

In this work, we present the results of experimental study of transient photovoltage (TPV) and photoelectric characteristics of the PSCs. The triple cation perovskite layers obtained by one-step deposition method from the precursor solution were used in the formed solar cells (see [2] for the detail). The TPV of the PSCs were measured using of 7 ns laser pulses at a wavelength of 532 nm.

Fig.1 presents the temporal profiles of photovoltage induced across two PSCs smples with diferent concentrations of Cs in perovskite layer.

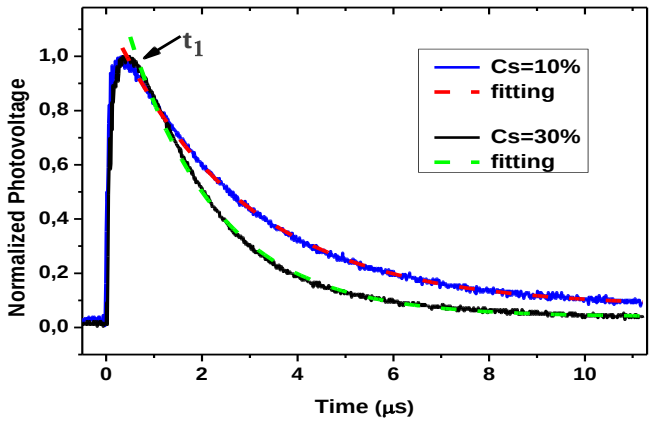


Fig. 1. Photovoltage decay transients of the solar cells with different concentrations of Cs in perovskite layer. Excitation laser power density 1.4 mW/cm^2

The photovoltage curves consist of a fast rising part, which, when reaching the maximum, is followed by a slow decaying part. The photovoltage reaches its maximum value with a delay of approximately 100 to 200 ns after laser excitation. The delay is defined by the time of electron transport in the perovskite layer. It is seen that, in a certain interval of time ($t > t_1$), the decay of the TPV can be approximated as a exponential function $U_{ph} = U_{ph0}\, e^{-t/\tau}$, where U_{ph0} is the value of U_{ph} at time t_1 and τ is the characteristic decay time constant.

Thus, the experimental results obtained in this work show that using the transient photovoltage method, it is possible to study the parameters of perovskite solar cells.

[1] E. H. Jung*et al.*, Nature 2019, 567, 511.
[2] S. Ašmontas, *et al.,* Materials 2022, 15, 1936

Development of an ionizing radiation detector based on CdZnTe-sensor for dosimetry

O. Banzak, H. Banzak

State University of Intellectual Technologies and Communications, street of Kuznechnay, 1565020, Odessa, Ukraine.

The development of modern detection units designed to monitor the state of protective barriers by measuring the dose rate of gamma radiation in the air, as part of NPP radiation monitoring systems, is an important and urgent task.

The use of CdZnTe to measure the dose rate is hampered by the fact that the sensitivity of the detector depends on the energy of gamma radiation and varies by more than 10 times [1]. To reduce the error due to the energy dependence of the sensitivity (ESD) of the CdZnTe sensor, digital correction of the output signal is used [2].

Let us recall the conclusions made earlier on the basis of studies of CdZnTe crystals. Sensors based on such crystals have low operating voltages, which “blurs” the lines of the measured spectrum. To eliminate this disadvantage and reduce the noise of the sensor, the crystals should be subjected to the thermal field treatment described above. This makes it possible to stabilize the main parameters of the crystals, increase the operating voltages by a factor of 2...3, and thereby reduce the sensor noise by a factor of 5...8. When such crystals are used in gamma radiation absorbed dose meters, the energy resolution reaches 20...40 keV.

When deciding on the geometry of a crystal, it should be taken into account that the inner part of its volume does not contribute to the photopeak: it is mainly the near-electrode regions that work. Therefore, for crystals with small values and ratio, the quasi-cylindrical geometry of the detector is optimal. Such sensors have the best ratio of sensitivity and resolution.

Based on the developed model, an ionizing radiation detector for dosimetry has been created. Its fundamental difference from known devices is the use of CdZnTe-crystals as a primary converter of gamma radiation (sensor). The advantages of such a solution, proven by previous studies, made it possible to create a detector that has:

− high resolution, no more than 40 keV;

− a wider dynamic range of values of the registered radiation dose rate – from background to emergency modes of reactor operation;

− lower value of the energy equivalent of noise.

When creating such a detector, the important problem of correcting the energy dependence of sensitivity (EDS) was solved. For this, a model has been developed that relates the frequency of pulses at the output of the detection unit to the energy of the detected radiation. The algorithm proposed in it allows ESP correction with an error of less than 7% for radiation energies from 20 keV to 1.5 MeV.

On this basis, a block diagram was proposed and a sample of a dosimetric detection unit with digital correction of the EDS was developed. In terms of design and output signals, it is compatible with BDMG-04, 08, 41 and can be used in any systems of AKRB NPP.

[1] Банзак О.В. Полупроводниковые детекторы нового поколения для радиационного контроля и дозиметрии ионизирующих излучений / О.В. Банзак, О.В. Маслов, В.А. Мокрицкий: Под ред. В.А. Мокрицкого, О.В. Маслова. – Монография. – Одесса, 2013. – Изд-во «ВМВ». – 220 с.

[2] Banzak O.V. CdZnTe sensors in the gamma-radiation dosimeter / O. V. Banzak, H. V. Banzak, O.I., Leschenko, K.S. Ganja / The 7th International scientific and practical conference “Scientific progress: innovations, achievements and prospects” (April 3-5, 2023) MDPC Publishing, Munich, Germany. 2023. P. 147 – 151.

Phase retrieval for arbitrary complex-valued objects using structured illumination

A.V. Kuzmenko[1], and O.M. Butok[2]

[1] *Branch of Applied Optics, Institute of Physics of National Academy of Sciences of Ukraine, Kyiv, Ukraine,*
[2] *Institute for Information Recording of National Academy of Sciences of Ukraine, Kyiv, Ukraine*

A method to solve of the phase retrieval problem in the non-convex formulation has been proposed for complex-valued objects with the support constraint [1,2]. It has been shown that two coded diffraction patterns (CDPs) obtained in the same Fresnel or Fraunhofer diffraction plane by masking the object with two, direct and inverse, random binary amplitude masks are sufficient to reconstruct an arbitrary complex-valued object with an accuracy to the global phase. The general solution of the problem was found as the sum of two mutually phase-consistent partial solutions obtained by applying the modified error-reduction (ER) or hybrid input-output (HIO) algorithm to each of two "mask + CDP" pairs.

The successful noise-resistant retrieval of images of various types complex-valued objects with an accuracy to the global phase was obtained for the oversampling ratios $\sigma \geq 2$ — in particular, σ = 4, 3, and 2 — and using a relatively small number of iterations. The influence of the degree of noisiness of the initial data by noises of various types on the process of restoring objects is also studied.

The proposed method and the results obtained were compared with the solution methods and experimental results presented in the works [3,4], which, like ours, is devoted to the issue of minimizing the number of masks needed to solve the CDI problem. Summarizing, we can say that due both to the use of structured illumination and to the performance of the modified ER and HIO algorithms, our method may be used to recovery a complex object in a simple and effective way for coherent radiation of any type, up to X-rays.

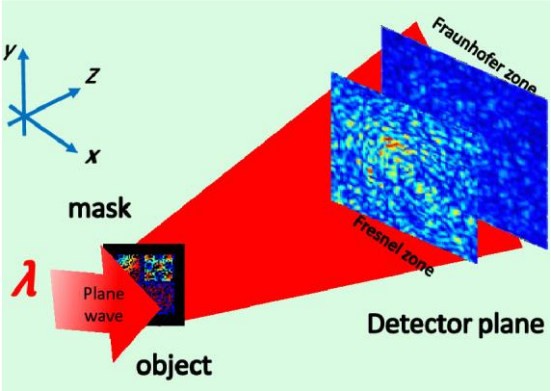


Fig. 1. A typical scheme for structured illuminations in diffraction imaging using a mask: the plane coherent wave (λ) illuminates the mask + sample pair, encoded diffraction pattern is measured by a detector in Fresnel or Fraunhofer plane.

[1] A.V. Kuzmenko and O.M. Butok. Phase retrieval for arbitrary complex-valued objects using structured illumination**.** https://doi.org/10.1364/opticaopen.22639216.v1
[2] Y. Shechtman, Y. C. Eldar, O. Cohen, H. N. Chapman, J. Miao, and M. Segev. Phase Retrieval with Application to Optical Imaging: A contemporary overview. IEEE Sig. Proc. Mag. 32, N 3, 87-109 (2015).
[3] US patent #11,237,059 B1 by Ersoy (2022).
[4] R. W. Gerchberg. A new approach to phase retrieval of a wave front. J. Mod. Opt. **49**, N 7, 1185-1196 (2002).

Optical rotation in the LBO and KTP nonlinear crystals

M. Shopa[1], N. Ftomyn[2]

[1] *Department of Atomic, Molecular and Optical Physics, Gdańsk University of Technology, Narutowicza 11/12, Gdańsk, 80-233, Poland*
[2] *Faculty of Physics, Ivan Franko National University of Lviv, Kyrylo & Mephodiy 8, Lviv 79005, Ukraine*

We have applied the modified high-accuracy polarimetric method [1,2], exploiting simultaneous polarization state measurement for two neighboring wavelengths of 633 and 661 nm, for the characterization of a nonlinear lithium triborate (LBO) and potassium titanyl (KTP) biaxial crystals.

The LBO mm^2 biaxial crystal from the group of borates is a well-known nonlinear optical material with a wide transparent range and high damage threshold. The class of orthorhombic crystals with mm2 point-group symmetry includes a series of common second-harmonic generating materials with relatively strong nonlinearity, in particular KTP and its isomorphous materials from the KTP family, including KTA, RTP and RTA.

Optical activity (OA) causes slight wavefront distortion when light propagates in an optically birefringent crystal section. Complementing the OA data for nonenantiomorphous crystals can be valuable, and not only for physical optics scholars.

The optical rotatory power of LBO crystals, as a measure of OA, according to the results of work by [3], is less than 1^o mm^{-1}. Authors of [3], probably, did not take the mismatch of the crystallographic and optical coordinate systems for LBO into account, which lead to incorrect data on the optical rotatory power. Our results of ORP for light propagation along one of the optical axes is 7.06^o mm^{-1}. Using known data on the structure and the electronic polarizability volumes, the measured values have been confirmed with calculations of optical rotation.

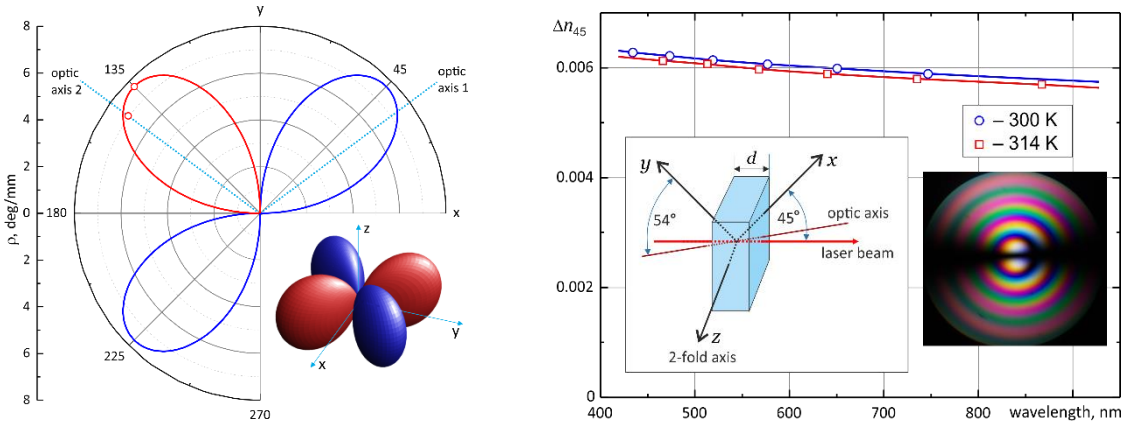


Figure 1. (Left) The calculated cross sections of the gyration surface in the xy plane in terms of the ORP (solid lines), and two experimental points (open circles). The fourth quadrant shows the full drawing of the gyration surface for the mm^2 crystal class. Red and blue colors correspond to positive and negative ORP values, respectively. (Right) Dispersion of the birefringence Δn_{45} at temperatures of 300 and 314 K with the crystal sample in relation to the crystallographic axes and a conoscopic interference pattern observed in white light along one of two optical axes shown in the insets.

[1] Shopa, Y., Shopa, M. & Ftomyn, N. (2023). J. Appl. Cryst. 56, 432–438
[2] Shopa, M., Shopa, Y., Shribak, M., Kostenyukova, E., Pritula, I. & Bezkrovnaya, O. (2020). J. Appl. Cryst. 53, 1257–1265.
[3] Etxebarria, J., Ortega, J. & Folcia, C. L. (2007). J. Appl. Cryst. 40, 919–923.

Investigating Hot Carrier Effects in GaAs P-N Diodes under Pulsed Laser Irradiation

I. Zharchenko[1], O. Masalskyi[1,2], J. Gradauskas[1,2], S. Ašmontas[1], A. Sužiedėlis[1], A. Šilėnas[1], A. Čerškus[1,3], A. Rodin[4]

[1] *Laboratory of Electronic Processes, Center for Physical Sciences and Technology, Lithuania,*
[2] *Department of Physics, Vilnius Gediminas Technical University, Lithuania*
[3] *Department of Mechatronics, Robotics and Digital Manufacturing, Vilnius Gediminas Technical University, Lithuania*
[4] *Laboratory of Solid State Lasers, Center for Physical Sciences and Technology, Lithuania*

The Shockley-Queisser theory states that photons with energy below the forbidden energy bandgap of a semiconductor do not contribute to the net photoresponse of a solar cell, while photons with energy higher than the bandgap participate in the formation of photoresponse [1]. However, recent investigations have revealed that photons with energy lower than the bandgap can induce a photovoltage across a p-n junction known as the hot carrier photovoltage, which exhibits an opposite polarity as compared to the classical photovoltage [2]. Our calculations have shown that up to 10% of the total absorbed solar light in GaAs falls within the below bandgap range, and this proportion strongly depends on carrier concentration and thickness of the top layer [3]. This research sheds light on the intricate interplay between the sub-bandgap photon absorption and its potential impact on solar cell performance, offering new insights for the design and optimization of photovoltaic devices.

This investigation examines photoresponse of LPE-grown GaAs p-n diodes to pulsed laser irradiation of varying wavelengths, specifically 0.532 μm, 1.064 μm, and 1.342 μm. The obtained results yield significant observations. First, the 1.342 μm photons (hν = 0.92 eV) predominantly contribute to the hot carrier current, displaying limited capacity to induce substantial classical generation-based photoresponse. Second, the influence of 1.064 μm photons (1.16 eV) leads to a prevailing hot carrier photoresponse that surpasses the classical photocurrent generated via the two-photon absorption. The heating effect arises due to the 0.9 eV excess energy remaining after generating the standard electron-hole pair, and contributes additionally to carrier heating via the intraband absorption. Third, in contrast to predictions based on classical theory, laser illumination with a 0.532 μm wavelength (hν = 2.32 eV, surpassing the bandgap) still exhibits a discernible hot carrier photoresponse which is likely caused by the 0.9 eV excess energy remaining after the classical single photon interband absorption. Overall, this study highlights significant role of the hot carrier effect and emphasizes its consideration when evaluating efficiency of solar cell. These findings challenge the conventional understanding derived from classical theory.

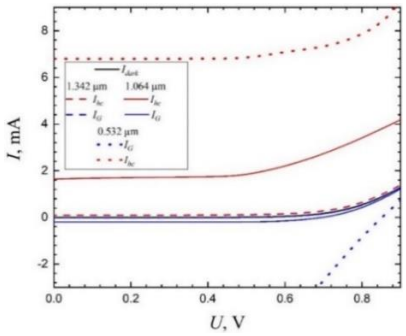


Fig.1. *I-V* characteristics of GaAs p-n junction under laser illumination of 0.4 MW/cm^2 intensity and corresponding wavelength: 0.532 μm (dotted lines), 1.064 μm (solid lines) and 1.342 μm (dashed lines). Red lines refer to the hot carrier photocurrent, blue lines denote classical generation-caused photocurrent.

[1] W. Shockley, H. J. Queisser, Detailed Balance Limit of Efficiency of p-n Junction Solar Cells, J. of Appl. Phys. 32, 510-519 (1961).
[2] S. P. Ašmontas, J. Gradauskas, D. Šeliuta, Photoelectrical properties of nonuniform semiconductor under infrared laser radiation, Nonresonant Laser-Matter Interaction conference, Proc. SPIE 4423, 18-27 (2000).
[3] O. Masalskyi, J. Gradauskas, Pre-themalizational effect of hot carriers on photovoltage formation in a solar cell, Ukr. J. Phys. Opt. 23, 117-125 (2022).

Topic VI: Lasers in nanotechnologies:

- Cluster, nanotubes and nanoparticles formation;
- Nanosized processing and structuring;
- Nanosized diagnostics.

Two copropagating laser beams in the excitation and characterization of slowly evaporating microdroplet

Y. Shopa[1], D. Jakubczyk[2], G. Derkachov[2], M. Kolwas[2], I. Kamińska[2], T. Wojciechowski[2]

[1] *Cardinal Stefan Wyszyński University in Warsaw, Warsaw, 01-815, Poland*
[2] *Institute of Physics, Polish Academy of Sciences, Warsaw, 02-668, Poland*

Luminescent nanoparticles (LN) Gd_2O_3: 1% Nd^{3+} in tetra ethylene glycol were used as nanoprobes to investigate the evolution of slowly evaporating free microdroplets of light-absorbing suspension. The levitating microdroplet was illuminated with two perpendicularly polarized CW laser beams of two wavelengths: 805 nm (IR, 1.6 W, p-polarized) and 660 nm (red, 50 mW, s-polarized). The IR beam was used for luminescence excitation while the red was for light scattering measurement. Both beams were vertically copropagating down a linear electrodynamic quadrupole trap equipped with two electrodes perpendicular to the trap axis.

Electrically charged droplets were confined horizontally with the quadrupolar AC field of rod electrodes, while vertical confinement was achieved with the DC field of plate electrodes. The levitating microdroplet was also backlit with a 1W red LED and its (vertical) position was observed as a shadow with a digital camera with a ~1.0 μm/pixel resolution.

In order to obtain a measurable luminescence signal, the IR laser beam was mildly focused. In consequence, it could exert significant forces: gradient, photophoretic or both. The luminescence of Nd^{3+} ions on 6 closely located spectral lines: 879, 892, 894, 911, 927 and 942 nm was used for optical probing of the interior of the microdroplet. Three concentrations (1, 10 and 50 mg/ml) of the nanoparticles were used and correspondingly analyzed (among others): (i) a very significant increase in modulation depth accompanied by a narrowing of spherical cavity resonance maxima (morphology-dependent resonances – MDRs) observed both in luminescence and scattering, (ii) the abrupt changes in the ratio between the luminescence and the scattering and (iii) the bi-stability in luminescence signal [1]. We attributed the observed phenomena to the interaction of optical MDRs with nanoparticles lattice shells forming and changing structure at the microdroplet surface. In this way, the formation and collapse of such lattices could be detected.

Using a photon counter coupled with a digital correlator (a system similar to that used in [2]), measurements of the intensity of light scattered on a micro-droplet as a function of time were carried out autocorrelation functions were obtained with the IR laser off and on. It was noticed that at a relatively high (~50 W/mm^2) power density of IR beams, absorbing LN (∅ 460 nm, concentration 5 mg/ml) rotates inside the micro-droplet with a characteristic time of ~$3\cdot10^{-4}$ s. The transition to the state of undisturbed suspension is rapid, after which the characteristic times are 0.1 s, and the fluctuations of the intensity of the scattered light increase significantly (t > 270 s).

[1] Y. Shopa, M. Kolwas, I. Kamińska et al. *JQSRT*, 108439, (2022).
[2] G. Derkachov, D. Jakubczyk, K. Kolwas, K. Piekarski, Y. Shopa, M. Woźniak, *Measurement*, 158, 107681, (2020).

Structural and optical properties of the nanoparticles of ZnTMO (TM: Co, Cr) generated by pulsed laser ablation in liquids and ultrasound wave-assisted

I. D. Stolyarchuk[1], O. O. Dan'kiv[1], A. I. Stolyarchuk[1], Yu. A. Pryima[1], O. V. Kuzyk[1], A. Medvids[2], V. D. Popovych[1], I.V. Hadzaman[1]

[1] *Department of Physics and Information Systems, Drohobych Ivan Franko State Pedagogical University, 24 I.Franko str., 82100 Drohobych, Ukraine.*

[2] *Institute of Technical Physics, Riga Technical University, 3/7 Paula Valdena str., LV-1048 Riga, Latvia*

Pulsed laser ablation in liquids (PLAL) has attracted recently much attention because of its advantage for fabrication of semiconductor nanoparticles compared to the other growth routes. Our previous application of this technique for preparation of ZnMnO and ZnCoO diluted magnetic semiconductor (DMS) nanoparticles has revealed peculiarities of the obtained nanostructures [1, 2]. The external environment greatly influences the process of laser ablation in liquid LAL. In the past decade, various LAL techniques have been developed, such as temperature field-assisted LAL, electric or magnetic field-assisted pulsed laser ablation in liquid and electrochemistry-assisted pulsed laser ablation in liquid [3].

In the present work, experimental investigations on structural and optical properties of the ZnTMO (TM: Co, Cr) nanoparticles generated by PLAL with ultrasound wave-assisted are reported.

The target was irradiated using a frequency-quadrupled Q-switched Nd:YAG pulsed laser, operating at 10 Hz with pulse width of 7 ns. Laser fluence was changed in range of (1-3) J/cm2. The target was immersed in bidistilled water inside a glass vessel. In the process of fabricated of the nanostructures the ultrasound with frequence from 0.2 to 2.0 MHz was also used. The colloidal aqueous solution with nanoparticles and appropriate layers onto Si and Al substrates were characterized using X-ray diffraction (XRD), scanning electron microscopy (SEM) and atomic force microscopy (AFM). In addition, the optical absorption and photoluminescence spectra were measured.

[1] Savchuk A. I. et al, Appl. Surf. Sci. 302 (2014), 205−208.
[2] Savchuk A. I. et al, Journal of Nano- and Electronic Physics 7(3) (2015), 03003.
[3] J. Xiao et al., Progress in Materials Science 87 (2017), 140–220.

Linear quantum molecule formed from three spherical quantum dots

V. B. Holskiy, M. D. Markanytsch, S. V. Holska

Department of Physics, Drohobych Ivan Franko State Pedagogical Univetsity,
24 I.Franko str., 82100 Drohobych, Ukraine.
(hol.wit@gmail.com)

The improvement of the technology for obtaining nanoheterosystems made it possible to obtain systems with closely spaced quantum dots. The spin [1] or charge [2] properties of the degrees of freedom can be used to create a quantum computer. Information carriers will be electrons, holes and excitons. Systems with three closely spaced QDs are promising in this direction. Nanosystems consisting of three tunnel-connected quantum dots or "triatomic" artificial molecules make it possible to study interesting phenomena related to electrostatics and molecular states of a triple quantum molecule (QM). Experimentally, molecules from quantum dots are intensively studied [3-5]. There can be two [3], three [4], four [5] or more nanocrystals in the QM. If we consider the geometry of the molecule, it can be linear [5] or triangular [4]. In turn, the first can be symmetrical, when the distances between QDs are the same, and not symmetrical.

This work is devoted to the study of the energy spectrum of an electron in a linear molecule of three spherical quantum dots. The electron Hamiltonian in the approximate effective mass for this nanosystem has the form:

$$\hat{H} = -\frac{\hbar^2}{2}\nabla\frac{1}{m}\nabla + U(r), \tag{1}$$

$$\text{where } U(r) = \begin{cases} 0, & \text{if } r \text{ the area of the matrix is traversed} \\ U_0, & \text{if } r \text{ found in the region QD} \end{cases}, \tag{2}$$

m — the effective mass of the electron for the corresponding region, $U_0 < 0$.

The approximation of the linear combination of quantum well orbitals was used to solve the problem. The wave function is represented as a linear combination of the electron wave functions of individual QDs.

The paper examines the stationary states of an electron in a molecule formed from a QD of a spherical shape of the system $InAs/GaAs$. The effective mass of an electron in these materials is $m_{InAs} = 0,027m_0$ and $m_{GaAs} = 0,067m_0$. And the band gap in this heterosystem, which determines the depth of the potential well, is equal to 700 meV. Considered QDs of such sizes that one bound electronic state existed in them. The range of radii of such nanocrystals of the selected system should vary from 16 to 32 $\overset{0}{A}$. The dependences of electron energy on CD sizes and distances between them are plotted.

[1] Loss D. and DiVincenzo D.P.. 1998 Phys. Rev. A 57, 120.
[2] Xin-QiLi and Arakawa Y. 2000 Phys. Rev. A 63, 012302.
[3] Johnson A. C., Petta J. R., et al. 2005 Phys. Rev. B 72, 165308.
[4] Rogge M.C., Haug R.J. 2008 Phys. Rev. B 78, 153310.
[5] Amaha S., Hatano T., et al.. 2010 Physica E 42 899–901.

The spatio-temporal temperature redistribution in the film under the influence of pulsed laser irradiation

O. V. Kuzyk[1], O. O. Dan'kiv[1], I. D. Stolyarchuk[1], R. M. Peleshchak[1,2], V. Kuhivchak[1], M. Sharafan[1], A. Medvids[3]

[1] *Drohobych Ivan Franko State Pedagogical University, Ukraine*
[2] *Lviv Polytechnic National University, Ukraine*
[3] *Riga Technical University, Latvia*

Recently, the subject of research is the modification of the surface of solid bodies under the influence of pulsed laser radiation. Laser-modified nano- and microstructures are created on the surface of metals, semiconductors, dielectrics and are formed in a significant time interval of the pulse duration. Laser-induced structuring can include both complete removal of the film and modification of its internal structural or electronic state [1]. On the other hand, films are the basis for many applications in the field of optical devices, photovoltaics and modern laser technologies. Optimizing these optical coatings requires a deep understanding of various linear and nonlinear mechanisms of interaction of pulsed radiation with matter.

An important stage in the process of forming nanostructures under the influence of pulsed radiation is the emergence of a temperature gradient [2] and its spatial-temporal redistribution in the irradiated film.

An important problem in predicting the results of the influence of laser irradiation is that, depending on the power and duration of the pulse, the different regions of the irradiated film may be in different aggregate states. To find the temperature distribution, in most cases, the thermal conductivity equation is solved, where the thermal conductivity coefficient and specific heat capacity do not depend on time [3]. However, during pulsed laser irradiation, not only nonuniform heating in the deep of the crystal occurs, but different phases can exist simultaneously, the boundaries of which shift over time.

This work proposes a method for calculating the spatio-temporal temperature redistribution under the influence of pulsed laser irradiation in the film and substrate, taking into account self-consistent boundary conditions. This model takes into account the possibility of the existence of several phases and the shift of their boundaries with time, the duration and the power of the laser pulse. The proposed model also makes it possible to analyze the influence of the substrate, in particular, in the case of the mismatch of lattice parameters of the contacting materials, on the process of heat propagation in the film and the substrate.

Within the framework of the developed model, the analysis was carried out and the criteria for the possibility of self-organization of point defects (interstitial atoms and vacancies) occurring in the irradiated semiconductor film were established. The influence of the mismatch between the lattice parameters of the film and the substrate and the conditions for the formation of self-organized nanostructures were investigated.

[1] Bonse J., Krüge J. Structuring of thin films by ultrashort laser pulses. Appl. Phys. A 129, 14 (2023).
[2] Kaupužs J., Medvidsa A., Onufrijevsa P., Mimura H. Optics and Laser Technology 111, 121–128 (2019).
[3] Myers T.G., Hennessy M.G., Calvo-Schwarzwälder M. The Stefan problem with variable thermophysical properties and phase change temperature. International Journal of Heat and Mass Transfer 149, 118975 (2020).

Study of local free volume under the influence of UV light in vegetable oil-based polymers

T. Kavetskyy[1,2], D.P. Královič[3], O. Šauša[2,3], P. Kalinay[2], H. Švajdlenková[4], I. Donchev[5], O. Smutok[6], V. Soloviev[7], J. Ostrauskaite[8], A. Kiv[5,9]

[1]*Drohobych Ivan Franko State Pedagogical University, 82100 Drohobych, Ukraine*
[2]*Institute of Physics, Slovak Academy of Sciences, 84511 Bratislava, Slovakia*
[3]*Department of Nuclear Chemistry, Comenius University in Bratislava, 84215 Bratislava, Slovakia*
[4]*Polymer Institute, Slovak Academy of Sciences, 84541 Bratislava, Slovakia*
[5]*South-Ukrainian K.D. Ushynsky National Pedagogical University, 65020 Odesa, Ukraine*
[6]*Department of Chemistry and Biomolecular Science, Clarkson University, 13699 New York, USA*
[7]*Kryvyi Rih State Pedagogical University, 50086 Kryvyi Rih, Ukraine*
[8]*Kaunas University of Technology, 50254 Kaunas, Lithuania*
[9]*Department of Materials Engineering, Ben-Gurion University of the Negev, 84105 Beer-Sheva, Israel*

A local free volume of acrylate epoxidized soybean oil (AESO) and vanillin dimethacrylate (VDM) in the presence or absence of a photoinitiator (PI) under the influence of UV light was investigated [1, 2]. The local free volume and its homogeneity in the cured mixtures were characterized using the positron annihilation lifetime spectroscopy (PALS) technique. The in-situ temperature measurement of the continuously irradiated AESO/VDM-based samples provides information about the kinetics. These experiments were carried out in PALS chamber with a fixed thermocouple (TC) in the middle of the reaction system and UV light from the bottom side. Due to two reaction systems with or without PI, two different flux densities of 0.7 and 22.2 $mWcm^{-2}$ of UV light were used, respectively, to achieve a similar temperature response.

It was found that increasing the content of VDM, which contains aromatic rings, caused a decrease in the local free volume of the cured polymer network, with consequences for the diffusion properties of the polymer, which were tested for the case of water. Another consequence of increasing the content of VDM was a decrease in the conversion of double bonds in the finally cured samples, characterized by NIR spectroscopy. This finding illustrates a case where the decrease in free volume is not necessarily related to an increase in the crosslinking density of the polymer, but is a consequence of the presence of an increase in the occupied volume of aromatic rings in the volume of the polymer.

Complex network methods approach, previously developed for plastic deformation dynamics in metals [3], was applied to study the in-situ photopolymerization kinetics in the selected AESO/VDM samples with or without PI based on the experimental data of PALS and TC. The modeling results are found to be in a good agreement with experimental observations, providing more insight on the in-situ reaction courses during illumination.

Acknowledgements
This work was supported in part by the Ministry of Education and Science of Ukraine (projects Nos. 0122U000850 and 0122U000874), National Research Foundation of Ukraine (project No. 2020.02/0100), and Slovak Research and Development Agency (project No. APVV-21-0335). T.K. also acknowledges the SAIA for scholarship in the IPSAS in the framework of the National Scholarship Programme of the Slovak Republic.

References

[1] D.P. Královič, K. Cifraničová, O. Šauša, H. Švajdlenková, T. Kavetskyy, A. Kiv. The process of photopolymerization of acrylated soybean oil-based epoxides investigated by positron annihilation lifetime spectroscopy, *Chemical Papers*, 2023, https://doi.org/10.1007/s11696-022-02607-0.
[2] D.P. Královič, K. Cifraničová, H. Švajdlenková, D. Tóthová, O. Šauša, P. Kalinay, T. Kavetskyy, J. Ostrauskaite, O. Smutok, M. Gonchar, V. Soloviev, A. Kiv. Effect of aromatic rings in AESO-VDM biopolymers on the local free volume and diffusion properties of polymer matrix, *Eur. Polym. J.*, 2023, submitted.
[3] A. Kiv, A. Bryukhanov, V. Soloviev, A. Bielinskyi, T. Kavetskyy, D. Dyachok, I. Donchev, V. Lukashin. Complex network methods for plastic deformation dynamics in metals, *Dynamics*, 2023, V.3, P.34-59.

Topic VII: Biomedical laser applications:

- Laser applications in medicine;
- Laser applications in biological systems.

Features of laser powder bed fusion additive manufacturing and post-processing of Co-Cr dental prosthesis

D.A. Lesyk[1,3,4*], O.S. Lymar [2], V.V. Dzhemelinskyi[1], D. Grzesiak[4], B. Powalka[4]
(*lesyk_d@ukr.net)

[1] *Laser Systems and Advanced Technologies Department, National Technical University of Ukraine "Igor Sikorsky Kyiv Polytechnic Institute", 03056 Kyiv, Ukraine*
[2] *MS Systems UA, 04050 Kyiv, Ukraine*
[3] *Physical Principles for Surface Engineering Department, G.V. Kurdyumov Institute for Metal Physics of the NAS of Ukraine, 03142 Kyiv, Ukraine*
[4] *West Pomeranian University of Technology, 70310 Szczecin, Poland*

Paying attention to the extremely high relevance and need for modernization of existing manufacturing methods, it is important to conduct new research in the field of dentistry, developing new dental products with additive manufacturing technology. The purpose of this work is the application of laser 3D printing technology for the production of custom-designed metal dental prosthetics. Laser powder bed fusion (L-PBF) is the most promising laser-based additive manufacturing technology in digital dentistry.

Nickel alloys are practically not used in modern dentistry for dental products due to the risk of nickel allergy [1]. Titanium alloys are used for removable partial prosthetics or implants [2]. Cobalt-chromium alloys are most suitable for the manufacture of dental prostheses using additive manufacturing technology due to their low cost, good mechanical properties, and significant corrosion resistance [3]. Due to the high hardness and low toughness, the Co-Cr alloys are not used for casting or machining.

This work aimed to design and laser-based additively manufacture of a customized Co-Cr alloy dental bridge by the L-PBF technology according to the patient's data. Particular attention is paid to the study of the effects of the applied method of thermomechanical post-processing on surface properties.

SISMA MYSINT100 Dual Laser printer was used to fabricate the specimens and dental prosthesis parts using the high-purity cobalt chromium metal powder. The 6-unit framework of fixed dental prosthesis 3D model was developed using a Dental Wings 7 Series scanner. The laser 3D-fabricated dental prosthesis parts were subjected to stress-relieving heat treatment and sandblasting.

The mass fraction of chemical elements in the Co-Cr powder was examined by an EXPERT 3L–XRF high-precision analyzer. The surface texture observations were conducted using a REM-106I scanning electron microscope (SEM). The residual porosity on the light optical images (LOM) was statistically analyzed using the Image J152 software. The non-contact surface roughness measurements were performed by using a VK-X260K profilometer.

The results indicated that the thermomechanical post-processing method eliminated the surface defects and reduced residual tensile stresses, providing material density in the near-surface layer of about 99.993% and required surface texture/roughness parameters according to the ceramic material imposition requirements.

[1] Ni, J., et al.: Three-dimensional printing of metals for biomedical applications, Mater. Today Bio., 3, 100024 (2019).
[2] Velu, R., et al.: A comprehensive review on bio-nanomaterials for medical implants and feasibility studies on fabrication of such implants by additive manufacturing technique. Materials, 13, 92 (2020).
[3] Mergulhão, M.V., et al.: Perspective of additive manufacturing selective laser melting in Co-Cr-Mo alloy in the consolidation of dental prosthesis. In (Ed.), Biomaterials in Regenerative Medicine, pp. 161–185, IntechOpen (2017).

Laser circumcision in the treatment of phimosis

O. B. Priyma

Truskavets City Hospital, Truskavets, Ukraine

Introduction. Surgical treatment of the foreskin has long been part of clinical practice. In 30% of patients with untreated or late-treated phimosis, penile cancer was detected Circumcisio - a planned surgical intervention that belongs to "one-day surgery". Urgent circumcision is performed only in the presence of acute urinary retention caused by obliteration of the prepuce sac.

The history of circumcisio has undergone a certain evolution. The classical circumcision of the foreskin was replaced by circumcision with the help of an electric knife, diathermy, and therefore, laser technologies. We proposed and introduced our own laser method of circumcisio.

Materials and methods. Annually, up to 30-40 circumcisions are performed in the urological hospital of Truskavetsk City Hospital, which is up to 10% of the total number of patients operated on in the department. We have been using laser circumcision for the past 7 years.For this, we use a diode laser of the red spectrum with a wavelength of 940 nm, the power of the installation is 30 W. A laser beam with a power of 9-12 W was used. The domestic device "Lika-surgeon" (produced by "Photonik +" in Cherkasy) is in operation.

The contingent of patients consisted of male persons aged from 7 to 80 years.

Own technique: under intravenous or epidural anesthesia, after treatment of the operative field, dissection of both leaves of the foreskin was performed longitudinally from the opening of the prepuceal sac in the direction of the coronary furrow, without reaching the last 3-5 mm on the lateral surfaces of the penis. After antiseptic treatment of the head of the penis and the foreskin, the longitudinal frenulum to the coronary furrow was then dissected (cut off) with the same laser beam. Later, both leaves of the foreskin were cut off with a laser beam. In this way, two mirror-symmetric flaps of the foreskin were cut off. An almost perfect circular excision of the foreskin was obtained. Provisionally, 4 vicryl knotted hemostatic sutures were applied to adapt the wound edges of both leaves. Hemostasis was provided by the laser beam itself.

Results and their discussion: the average length of stay in the hospital was 1 day. Swelling of the foreskin and skin of the penis was absent or insignificant. Subcutaneous hematomas of the penis were not observed. The wound healed within 2 weeks. The rehabilitation period was 1 month.

Conclusion: 1. Laser circumcision using our own method is an effective method of treating phimosis. 2. Laser circumcision with a diode laser of the red spectrum with a wavelength of 940 nm and a beam power of 9-12 W provides a good cosmetic and functional effect and thorough hemostasis.

Measurement of oscillations of the grape snail organs using a laser vibrometer.

Y. Serozhkin, E. Venger, A. Sidnev

V.E. Lashkaryov Institute of Semiconductor Physics, Kyiv, Ukraine

The grape snail has long been one of the main objects of study for neurophysiologists. The reason for this was the simplicity of the snail's nervous system. However, recent studies have shown that, despite this simplicity, the snail has very complex behavioral functions.

The aim of the work is to study the oscillations of the snail organs, both in a free state and under external influence. The studies were carried out using a laser vibrometer.

Figure 1 shows the results of measurements of the snail head surface oscillations (left after the 0.1 Hz filter, right after the 200 Hz filter).

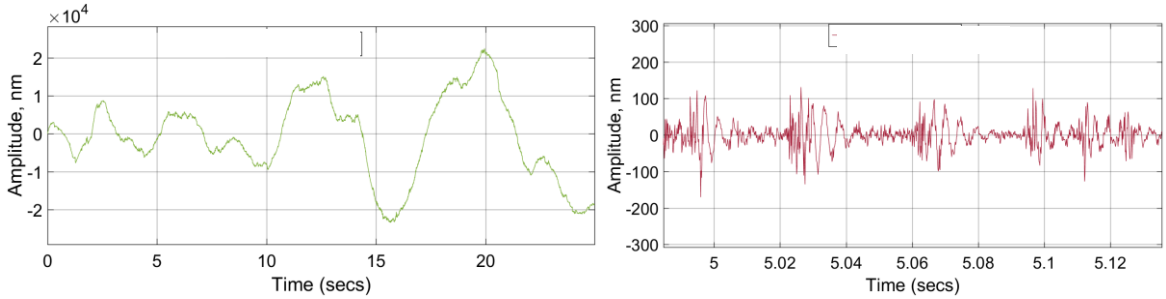


Figure 1. The snail head surface oscillations (left after the 0.1 Hz filter, right after the 200 Hz filter)

Figure 2 shows the results of measurements of oscillations of the surface of the snail's paw (left after the 0.1 Hz filter, right after the 200 Hz filter).

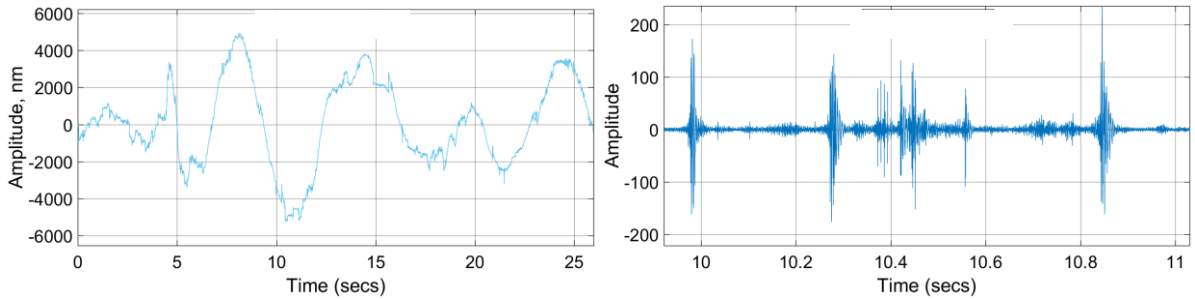


Figure 2. The results of measurements of oscillations of the surface of the snail's paw (left after the 0.1 Hz filter, right after the 200 Hz filter).

The amplitude of oscillations of the surface of the head is up to 20 microns, and the paws are up to 6 microns. These quasi-periodic oscillations are the movement of the head and paw as a whole. Of interest are the vibrations of the head surface in the frequency range above 200 Hz. These are almost periodic pack of pulses with a repetition frequency of about 30 Hz and an amplitude of about 100 nm.

CONTENTS

Topic 1. **PHYSICAL AND MATHEMATICAL FUNDAMENTALS OF LASER SYSTEMS** 4

A. Negriyko, V. Bezrodnyi, T. Bezrodna, L. Kosyanchuk, O. Antonenko 5
Laser elements based on dye-doped polyurethane matrices……..

B.V. Padlyak, I.I. Kindrat, R. Lisiecki, V.T. Adamiv
Laser materials based on borate glasses, co-doped by Er and Ag …… 6

O. Mys, D. Adamenko, I. Martynyuk-Lototska, and R. Vlokh
Enhancement of acousto-optic diffraction efficiency due to the ellipticity of optical eigenwaves caused by an external magnetic field and spontaneous electric polarization 7

I. Matsniev, V. Khodakovskyy, A. Negriyko 8
Compact diode-pumped Nd:YAG laser……..

A. Derzhypolskyi, L. Derzhypolska, A. Negriyko 9
M2 measurement based on long range focusing of laser beam……

I.I. Kindrat, B.V. Padlyak, R. Lisiecki, A. Drzewiecki, I.M. Teslyuk, V.T. Adamiv
Spectroscopy of the Tm-doped and Tm-Ag co-doped lithium tetraborate glasses ……. 10

R.Ya. Leshko, I.V. Bilynskyi, O.V. Leshko
Interlevel absorption of electromagnetic waves of the non-concentric spherical core-shell quantum dot …… 11

P. Potera, Ya. Zhydachevskii, D. Piwowarska, S.M. Kaczmarek
Stable color centers induced in $PbMoO_4$ crystals by gamma quanta irradiation ……. 12

Topic 2. **DEVELOPMENT OF LASERS AND LASER SYSTEMS** 13

L. Fedorenko, D. Korbutyak, A. Evtukh, V. Naumov, V. Yukhymchuk, P. Onufrijevs, A. Medvids, H. Mimura
Stimulated UV Emission of ZnO Powder with Coherent and Incoherent Feedback …… 14

Topic 3. **LASER PROCESSING OF MATERIALS** 15

A. Medvids, P. Onufrijevs, J. Kaupužs, J. Padgurskas, A. Zunda
Anatase or Rutile TiO_2 Formation on Ti by Laser Radiation: Mechanical, Photocatalytic and Antibacterial Properties …… 16

Yu. Nykyruy, B. Cieniek, I. Stefaniuk, S. Mudry 17
EMR study of the $Fe_{73.5}Si_{15.5}B_7Nb_3Cu_1$ amorphous ribbon modified by laser ……

W. Żyłka, B. Cieniek, I.Stefaniuk
The effect of laser radiation on the properties of paint components, studied using the EMR method …… 18

Topic 4. **LASER DEPOSITION** 19

B. Cieniek, I. Virt, I. Stefaniuk
Spectroscopic properties of nickel ions in $Zn_{0.99}Ni_{0.01}O$ thin film grown using PLD method …… 20

A. Barlowski, P. Ciupak, K. Zembrowska, P. Sagan, T. Jasinski, M. Kuzma
Self- aggregated nanoparticles of ZnCrTe formed by laser ablation …… 21

I.Virt, P. Potera, B. Cieniek
Pulsed laser deposition of carbon nanotube films …… 22

B. Cieniek, I. Virt, I. Rogalska, I. Stefaniuk
Spectroscopic properties of nickel ions in $Zn_{0.9}Cu_{0.1}O$ thin film grown using PLD method …… 23

Topic 5. **LASER TECHNICAL AND TECHNOLOGY APPLICATIONS** 24

V. Kadan, I.Pavlov, I. Blonskyi, T. Pavlova, Yu. Seriozhkin, A. Dmytruk
Sensitive measurements of two-photon absorption in semiconductors by combining Z-scan and loss modulation …… 25

L. Muravsky, Z. Nazarchuk, O. Kuts
Determining the size and depth of square planar subsurface defects in laminated composites by optoacoustic technique …… 26

S. Ašmontas, A. Čerškus, J. Gradauskas, A. Grigucevičienė, R. Juškėnas, K. Leinartas, A. Lučun, O. Masalskyi, M. Mujahid, K. Petrauskas, A. Selskis, A. Sužiedėlis, E. Širmulis
Laser induced photoresponse in perovskite solar cells …… 27

O. Banzak, H. Banzak
Development of an ionizing radiation detector based on CdZnTe-sensor for dosimetry 28

A.V. Kuzmenko, and O.M. Butok
Phase retrieval for arbitrary complex-valued objects using structured illumination … 29

M. Shopa, N. Ftomyn
Optical rotation in the LBO and KTP nonlinear crystals …… 30

I. Zharchenko, O. Masalskyi, J. Gradauskas, S. Ašmontas, A. Sužiedėlis, A. Šilėnas, A. Čerškus, A. Rodin
Investigating Hot Carrier Effects in GaAs P-N Diodes under Pulsed Laser Irradiation.. 31

Topic 6. **LASERS IN NANOTECHNOLOGIES** 32

Y. Shopa, D. Jakubczyk, G. Derkachov, M. Kolwas, I. Kamińska, T. Wojciechowski
Two copropagating laser beams in the excitation and characterization of slowly evaporating microdroplet …… 33

I. D. Stolyarchuk, O. O. Dan'kiv, A. I. Stolyarchuk, Yu. A. Pryima, O. V. Kuzyk, A. Medvids, V. D. Popovych, I.V. Hadzaman
Structural and optical properties of the nanoparticles of ZnTMO (TM: Co, Cr) generated by pulsed laser ablation in liquids and ultrasound wave-assisted …… 34

V. B. Holskiy, M. D. Markanytsch, S. V. Holska
Linear quantum molecule formed from three spherical quantum dots …… 35

O. Kuzyk, O. Dan'kiv, I. Stolyarchuk, R. Peleshchak, V. Kuhivchak, M. Sharafan, A. Medvids
The spatio-temporal temperature redistribution in the film under the influence of pulsed laser irradiation …… 36

T. Kavetskyy, D.P. Královič, O. Šauša, P. Kalinay, H. Švajdlenková, I. Donchev, O. Smutok, V. Soloviev, J. Ostrauskaite, A. Kiv
Study of local free volume under the influence of UV light in vegetable oil-based polymers…… 37

Topic 7. **BIOMEDICAL LASER APPLICATIONS** 38

D.A. Lesyk, O.S. Lymar, V.V. Dzhemelinskyi, D. Grzesiak, B. Powalka
Features of laser powder bed fusion additive manufacturing and post processing of Co-Cr dental prosthesis …… 39

O. B. Priyma
Laser circumcision in the treatment of phimosis …… 40

Y. Serozhkin, E. Venger, A. Sidnev
Measurement of oscillations of the grape snail organs using a laser vibrometer…… 41

ALPHABETICAL LIST..... 45

ALPHABETICAL LIST

A

Adamenko D. 7
Adamiv V.T.....6, 10
Antonenko O. 5
Ašmontas S.....27, 31

B

Banzak H. 28
Banzak O. 28
Barlowski A.....21
Bezrodna T. 5
Bezrodnyi V. 5
Bilynskyi I.V. 11
Blonskyi I. 25
Butok O.M.....29

C

Čerškus A. 27, 31
Cieniek B.....17, 18, 20, 22, 23
Ciupak P. 21

D

Dan'kiv O. O. 34, 36
Derkachov G. 33
Derzhypolska L. 9
Derzhypolskyi A. 9
Dmytruk A.....25
Donchev I. 37
Drzewiecki A.....10
Dzhemelinskyi V.V. 39

E

Evtukh A. 14

F

Fedorenko L. 14
Ftomyn N.....30

G

Gradauskas J.....27, 31
Grigucevičienė A.....27
Grzesiak D. 39

H

Hadzaman I.V.....34
Holska S. V. 35
Holskiy V. B.....35

J

Jakubczyk D. 33
Jasinski T. 21
Juškėnas R. 27

K

Kaczmarek S.M. 12
Kadan V. 25
Kalinay P. 37
Kamińska I. 33
Kaupužs J. 16
Kavetskyy T. 37
Khodakovskyy V. 8
Kindrat I.I. 6, 10
Kiv A. 37
Kolwas M. 33
Korbutyak D. 14
Kosyanchuk L. 5
Královič D.P. 37
Kuhivchak V. 36
Kuts O. 26
Kuzma M. 21
Kuzmenko A.V. 29
Kuzyk O. V. 34, 36

L

Leinartas K. 27
Leshko O.V. 11
Leshko R.Ya. 11
Lesyk D.A. 39
Lisiecki R. 6, 10
Lučun A. 27
Lymar O.S. 39

M

Markanytsch M. D. 35
Martynyuk-Lototska I. 7
Masalskyi O. 27, 31
Matsniev I. 8
Medvids A. 14, 16, 34, 36
Mimura H. 14
Mudry S. 17
Mujahid M. 27
Muravsky L. 26
Mys O. 7

N

Naumov V. 14
Nazarchuk Z. 26

Negriyko A. 5, 8, 9
Nykyruy Yu. 17

O

Onufrijevs P. 14, 16
Ostrauskaite J. 37

P

Padgurskas J. 16
Padlyak B.V. 6, 10
Pavlov I. 25
Pavlova T. 25
Peleshchak R. M. 36
Petrauskas K. 27
Piwowarska D. 12
Popovych V. D. 34
Potera P. 12, 22
Powalka B. 39
Priyma O. B. 40
Pryima Yu. A. 34

R

Rodin A. 31
Rogalska I. 23

S

Sagan P. 21
Šauša O. 37
Selskis A. 27
Seriozhkin Yu. 25
Serozhkin Y. 41
Sharafan M. 36
Shopa M. 30
Shopa Y. 33
Sidnev A. 41
Šilėnas A. 31
Širmulis E. 27
Smutok O. 37
Soloviev V. 37
Stefaniuk I. 17, 18, 20, 23
Stolyarchuk A. I. 34
Stolyarchuk I. D. 34, 36
Sužiedėlis A. 27, 31
Švajdlenková H. 37

T

Teslyuk I.M. 10

V

Venger E. 41
Virt I. 20, 22, 23
Vlokh R. 7

W

Wojciechowski T. 33

Y

Yukhymchuk V. 14

Z

Zembrowska K. 21
Zharchenko I. 31
Zhydachevskii Ya. 12
Zunda A. 16
Żyłka W. 18

Program

of the conference LTLA-2023

June 29 - June 30, 2023

Truskavets, Ukraine

Time: *(CEST)*	**Date** June 29, 2023, Thursday	*Time:* *(CEST)*	**Date** June 30, 2023, Friday
9:00÷9:15	**Ceremonial opening of the Conference**	9:00÷11:05	**Plenary sessions** Topic V, Topic VI, Topic VII.
9:20÷10:35	**Plenary sessions** Topic I, Topic II, Topic III.		
10:35÷11:00	Break time		
11:00÷12:40	**Plenary sessions** Topic IV.	11:05÷11:30	Break time
12:40÷1:45	Break time	11:30÷12:30	**Oral sessions** Topic VI, Topic VII.
1:45÷3:15	**Oral sessions** Topic I, Topic II.		
3:15÷3:45	Break time		
3:45÷5:00	**Oral sessions** Topic III, Topic IV, Topic V.	12:30÷12:45	**Closing Conference LTLA-2023**
5:00÷6:00	**Poster session** Topic I, Topic II, Topic III, Topic IV, Topic V, Topic VI, Topic VII.		

Link to launch conference :

https://teams.microsoft.com/l/meetup-join/19%3ameeting_ZTRhY2EyNzMtY2E3YS00MTllLTkxY2MtYWRkZmFkOTE3Mjkx%40thread.v2/0?context=%7b%22Tid%22%3a%2280f4c02e-2264-45f3-b124-20b24047d29b%22%2c%22Oid%22%3a%2272de1743-5728-41bd-bbbf-cc2439f902db%22%7d

Scientific Edition:
Ihor Virt

MATERIALS
OF INTERNATIONAL SCIENTIFIC
AND TECHNICAL CONFERENCE
LASER TECHNOLOGIES.
LASERS AND THEIR APPLICATION.
2023

Computer typing and
Sent to printing 22.06.23. Signed for printing 26.06.23.
Format 60´90/16. Offset paper. Times Font.
Number of copies 50. Printed sheets 10. Order №124.
Operational Center Print "SHVYDKODRUK"
st. D. Galician, 1, Drohobych, 82100
Tel. (0324) 41-08-90
e-mail: druksv@gmail.com